Ezrin-anchored PKA phosphorylates serine 369 and 373 on connexin 43 to enhance gap junction assembly, communication, and cell fusion

Aleksandra R. Dukic[1,2], Pascale Gerbaud[3], Jean Guibourdenche[4], Bernd Thiede[5], Kjetil Taskén[1,2,*] & Guillaume Pidoux[3*]

[1]Centre for Molecular Medicine Norway, Nordic EMBL Partnership, University of Oslo and Oslo University Hospital, Oslo N-0318, Norway; [2]K.G. Jebsen Centre for Cancer Immunotherapy, University of Oslo, Oslo N-0317, Norway; [3]UMR-S 1180, Inserm, Univ. Paris-Sud, Université Paris-Saclay, Châtenay-Malabry, France; [4]Department of Biosciences, University of Oslo, Oslo N-0317, Norway and [5]Department of Biological Endocrinology, CHU Cochin, AP-HP, Paris, France; Faculté de Pharmacie, Université Paris Descartes, Paris, France.

Running title: PKA phosphorylates Cx43 on serine 369 and 373

Keywords: Cell signaling, cAMP, cell fusion, ezrin, Cx43

*Correspondence to: kjetil.tasken@ncmm.uio.no and guillaume.pidoux@inserm.fr

Abstract

A limited number of human cells can fuse to form multinucleated syncytia. In the differentiation of human placenta, mononuclear cytotrophoblasts fuse to form an endocrinologically active, non-proliferative, multinucleated syncytium. This syncytium covers the placenta and manages the exchange of nutrients and gases between maternal and fetal circulation. We recently reported protein kinase A (PKA) to be part of a macromolecular signaling complex with ezrin and gap junction protein connexin 43 (Cx43) that provides cAMP-mediated control of gap junction communication. Here, we examined the associated phosphorylation events. Inhibition of PKA activity resulted in decreased Cx43 phosphorylation, which was associated with reduced trophoblast fusion and differentiation. *In vitro* studies using peptide arrays, together with mass spectrometry, pointed to serine 369 and 373 of Cx43 as the major PKA phosphorylation sites that increases gap junction assembly at the plasmalemma. A combination of knockdown and reconstitution experiments and gap-FLIP assays with mutant Cx43 containing single or double phosphoserine-mimicking amino acid substitutions in putative PKA phosphorylation sites demonstrated that phosphorylation of S369 and S373 mediated gap junction communication, trophoblast differentiation and cell fusion.

Introduction

Cell fusion is a crucial process in fertilization, placentation, skeletal muscle formation, bone homeostasis, and metastasis [1-5]. Cell fusion and syncytial formation involve mixing of cell content and plasma membrane components between two or more cells. In humans, placentation requires cell fusion of cytotrophoblasts (CTs) to form multinucleated syncytiotrophoblasts (STs) on chorionic villi that extend into the maternal blood circulation. These syncytia form an interface between the mother and the fetus that allows exchange of gases and nutrients necessary for fetal growth and development [6]. Furthermore, STs synthesize and secrete pregnancy-specific peptide hormones such as human chorionic gonadotropin (hCG) and human placental lactogen (hPL) [7, 8]. Similarly as observed *in vivo*, isolated mononucleated CTs aggregate and fuse *in vitro* to form non-proliferative, multinucleated STs that produce pregnancy-specific hormones [9]. Numerous proteins in tight junctions, adherens junctions, and gap junctions have been reported to control or be associated with the first steps of trophoblast fusion processes [10-12]. However, only syncytins present defined fusogenic properties in trophoblasts and in other cell fusion models [13-15].

The cAMP signaling pathway plays a critical role in induction of trophoblast fusion (reviewed in [16]). hCG signals in an autocrine or paracrine fashion via the G protein-coupled luteinizing hormone (LH) receptor (LH/CG-R). This stimulates cAMP synthesis and activates of protein kinase A (PKA) leading to phosphorylation or increased expression of fusogenic proteins (*e.g.* syncytins, cadherin, and connexin) [11, 17-19]. These cellular adaptations are critical to trigger CT fusion [16, 20].

A-kinase anchoring proteins (AKAPs) are a family of structurally diverse proteins with the ability to scaffold PKA [21, 22]. All AKAPs contain an A-kinase binding domain (AKB) that anchors PKA and a unique targeting domain to localize the PKA-AKAP complex to defined subcellular structures (*e.g.* membranes or organelles). Together these features of AKAPs confer the spatial regulation of PKA signaling events by controlling the phosphorylation of specific substrates [23-25]. Furthermore, AKAPs establish intracellular signalosome complexes by scaffolding additional signaling molecules (*e.g.* kinases, protein phosphatases, or cAMP phosphodiesterases), which add to the temporal regulation of PKA signaling [26, 27]. Finally, AKAPs bind to or co-localize with specific

PKA substrates to allow rapid and efficient phosphorylation [25]. Several AKAPs have been described in human placenta and we recently showed that two or more AKAPs are involved in the regulation of trophoblast fusion [20, 28-30]. Specifically, ezrin establishes a signaling complex with PKA and connexin 43 (Cx43) that mediates gap junction communication and thereby triggers trophoblast fusion [29, 31]. Ezrin belongs to the ERM (ezrin-radixin-moesin) family of proteins. These proteins are known to scaffold and organize anchored complexes with signaling effector molecules. The ezrin N-terminal domain contacts transmembrane proteins whereas the central region binds PKA through an AKB domain [32-35]. Recently, we provided evidence that the region encompassing amino acids 505 to 521 of ezrin located in the C-terminal domain, binds to the Cx43 gap junction protein [29] and that anchored PKA has a gate keeper function to regulate gap junction communication.

In vertebrates, communication between adjacent cells occurs through gap junctions, which are composed of connexin (Cx) hexamers forming gap junction channels in the plasma membrane. These intercellular channels allow diffusion of ions and small molecules (< 1kDa) such as cAMP, cGMP, inositol trisphosphate (IP_3), and Ca^{2+} [36]. Gap junctional intercellular communication (GJIC) facilitates the coordination of cell proliferation, cell differentiation, embryonic development, cell fusion, and the synchronized contraction of heart and smooth muscle [12, 37-40]. Cxs are a family of structurally related membrane proteins that in humans are encoded by 21 different genes [37, 38, 41]. Abnormal expression or sub-cellular distribution of gap junction proteins has been associated with several diseases such as cancer, deafness, neuropathy, and heart disease [38]. Cx43 is by far the most abundantly and widely expressed gap junction protein and it is noteworthy that Cx43 is the key gap junction protein expressed in fusion-competent human CTs [12, 18]. Cx43 allows the transfer from cell to cell of fusogenic signals that initiate cellular synchronization and organization of the fusogenic macrocomplex machinery in the right place and at the right time to trigger cell-cell fusion (for review [16]). While the N-terminal region of Cx43 represents two-thirds of the protein and docks with Cx in the adjacent membrane, which serves to form the pore, the C-terminal cytoplasmic region is more disordered and confers regulation of pore opening and conductivity [42]. Several kinases (*e.g.* PKA, AKT, PKC, CK1, MAPK and Src) phosphorylate Cx43 in the C-terminal domain thereby affecting gap junction trafficking, assembly, recycling or communication [43]. Furthermore, we identified a

region in the C-terminal domain of Cx43 encompassing amino acids R362 to D379 that binds ezrin and directs a pool of PKA to Cx43 [29, 31]. Interestingly, this sequence overlaps with a region that has been described to encompass several of the phosphorylation sites that regulate Cx43 function [44]. However, our previous study did not allow us to identify which of the putative single or multiple residues in the region 364 to 373 of Cx43 phosphorylated by PKA that trigger trophoblast fusion [29, 31]. Furthermore, the residues in Cx43 that are phosphorylated by PKA and the functional consequences of PKA phosphorylation have not been fully elucidated [45]. Therefore we aimed to identify the specific PKA phosphorylation sites in Cx43 that control gap junction assembly and communication and, thereby, cell fusion. We report here that the anchoring of PKA through the AKAP ezrin is necessary to provide spatiotemporal control of phosphorylation of S369 and S373 in Cx43. These phosphorylation events increase gap junction assembly and communication and thus human trophoblast fusion.

Experimental

Primary cultures of human placental trophoblasts

Villous cytotrophoblasts were isolated from term placentas and cultured as previously described [19]. Placentas were obtained from women aged between 28 and 44 years with uncomplicated pregnancies undergoing normal Cesarean sections at Cochin Port-Royal maternity unit (Paris, France) with written informed consent under Ethics Committee Approval CCPRB Paris Cochin n. 18-05.

Cell culture

The rat liver epithelial cell line IAR20 and HEK293 were cultured at 37°C and 5% CO_2 conditions in DMEM high glucose GlutaMAX medium (Life Technologies, Illkirch, France) supplemented with 10% fetal bovine serum (Life Technologies, Illkirch, France) and 1% PenStrep (Life Technologies, Illkirch, France).

Peptide synthesis and loading

Peptides used in trophoblast fusion, hormones and immunoblot assays were synthesized as previously described by [46]. Titrations of the optimal peptide concentration used (10 μM for Arg-tagged PKI or scrambled PKI control) and loading conditions (60 min for immunoblot assays and 48 h for fusion and hormone assays) for effective intracellular delivery (>95% w/o toxicity) was described previously [29].

Immunolocalization studies

Immunocytofluorescence was performed as previously described [10]. Fixed cells were first incubated with primary monoclonal antibody (2.5 μg) to desmoplakin (Abcam, Paris, France), Cx43 (Sigma-Aldrich, Courtaboeuf, France) and next with the appropriate fluorochrome-conjugated secondary antibody (Alexa Fluor 488 (1:500, Life Technologies, Illkirch, France)). Immunfluorescence microscopy pictures were taken using a 3D-deconvolution microscope (Leica, France). For each acquisition and wavelength z-stacks images were assembled and processed with ImageJ. Micrographs show a representative selected z from stacks.

115

116 **Trophoblast fusion assay**

117 Cell fusion was quantified by trophoblast fusion assays as previously described [10, 14]. Briefly,
118 syncytium formation was followed by monitoring the cellular distribution of desmoplakin and nuclei
119 after immunostaining. Desmoplakin staining at the boundaries of aggregated mononuclear cells
120 gradually disappears during syncytium formation. Cell nuclei were counterstained with DAPI-
121 containing mounting medium. From a random point in the middle of the coverslips, 1000 nuclei
122 contained in desmoplakin-delimited mononuclear cytotrophoblasts and syncytia were counted. Three
123 coverslips were examined for each experimental condition. Results are expressed as the number of
124 nuclei per syncytium. The fusion index was determined as (N—S)/T, where N is the number of nuclei
125 in the syncytia, S is the number of syncytia, and T is the total number of nuclei counted.

126

127 **Hormone assays**

128 hCG and hPL concentrations were determined as previously described [10].

129

130 **Protein sample preparation and immunoblot analysis**

131 Cell extracts were prepared as previously described [46]. Protein samples were resolved by SDS-
132 PAGE and immunoblotted with antibodies to PKA RIα (0.25 µg/ml), PKA RIIα (0.25 µg/ml, BD
133 Biosciences, Rungis, France); PKA Cα (1:1000), phospho-PKA substrate (RRXpS, 1:1000, Cell
134 signaling, Saint Quentin, France); ezrin (0.5 µg/ml), unphosphorylated Cx43 (0.5 µg/ml, Life
135 Technologies, Illkirch, France); actin (0.8 µg/ml), Cx43 (0.25 µg/ml), phospho-Connexin 43 (Ser373)
136 (1:1000, Invitrogen), AKAP18 (1 µg/ml, Sigma-Aldrich, Courtaboeuf, France), GFP-tag (1 µg/ml,
137 Clontech, Saint Quentin, France), turboGFP (1:1000, OriGene). After incubation with appropriate
138 DyLight Fluor-conjugated secondary antibody (680 or 800 conjugate, Life Technologies, Illkirch,
139 France), blots were revealed by using Odyssey infrared fluorescent system (Li-Cor, Bad Homburg,
140 Germany).

141

142 **Duolink™ Proximity Ligation Assay**

Interactions between ezrin, Cx43, PKA RIα, PKA RIIα, PKA Cα, desmoplakin, and GFP-tag in trophoblasts were analysed using the Duolink™ proximity ligation assay according to manufacturer's instructions. Pictures were taken using a 3D deconvolution microscope (Leica, France). For each acquisition and wavelength z-stacks were generated and processed with ImageJ. Micrographs show the average intensity of z projection of z-stacks. Quantification of protein proximity was performed by using ImageJ and by normalizing the intensity of fluorescence spots generated with the number of nuclei.

Immunoprecipitation

Antibodies (4 µg each) described above (anti-RIα, anti-RIIα, anti-Cα, anti-ezrin, anti-Cx43; anti-GFP-tag (Clontech, Saint Quentin, France) and nonspecific rabbit or mouse IgG (Jackson ImmunoResearch, Suffolk, UK)) were covalently coupled to protein G-linked Dynabeads (Life Technologies, Illkirch, France) using BS^3 (5 mM, Thermo Scientific, Illkirch, France). Cell lysates (200 µg proteins) were added to the bead-linked antibodies. Lysates represent 2.5% of output controls. Immunocomplexes were analyzed by LC MS/MS or immunoblotted with indicated antibody.

PKA activity assay

PKA phosphotransferase activity was assayed as previously described [47] with some modifications. Briefly, immunoprecipitations were performed and precipitates resuspended and incubated in a kinase reaction mix containing 10 mM ATP, 50 mM Tris-HCL pH 7.4, 1M MgAc2, [γ-^{32}P] ATP and Kemptide (Leu-Arg-Arg-Ala-Ser-Leu-Gly) with cAMP (5 µM) ± PKI (10 µM) for 9 min at 30 °C. The reaction mixture was spotted on phosphocellulose paper, washed 4 times in 75 mM phosphoric acid, once in 95% ethanol, filters were next dried and subjected to liquid scintillation counting.

Peptide array synthesis and phosphorylation

Peptide arrays were synthesized on nitrocellulose membranes using a MultiPep automated peptide synthesizer (Intavis Bioanalytical Instruments AG, Koeln, Germany) as described [48]. Briefly,

peptides encompassing amino acids V359 to R376 of the Cx43 C-terminal region in which single or multiple combination of serine substitution with alanine were synthetized and spotted on filters.

For *in vitro* PKA phosphorylation of peptide arrays, membranes were rinsed in 95% ethanol and washed in Tris-buffered saline with 0.1% triton X-100, then incubated with rotation for 30 min at 30 °C in a solution with 50 mM MOPS pH 6.8, 50 mM NaCl, 2 mM $MgCl_2$,1 mM DTT and 50 µM ATP (including 100 µCi/mL ([γ-^{32}P]ATP) with 0.3 mg/mL PKA. The membranes were subsequently washed four times in a buffer containing 1% sodium dodecyl sulfate (SDS), 8 M urea, 0.5% β-mercaptoethanol, four times in 50% ethanol with 10% acetic acid and two times in 95% ethanol before they were subjected to autoradiography. Films were next analyzed and quantified using ImageJ and Protein Array Analyzer plugin [49].

Protein identification by LC MS/MS

Protein identification in immunoprecipitates was performed by NanoLC-ESI-MS after tryptic digestion as described [50].

SiRNA, mammalian expression vectors and transfection

Transfections (siRNA and plasmids) were performed using Lipofectamine 2000 CD reagent (Life Technologies, Illkirch, France). SiRNA transfections described previously [10] were performed with Cx43 siRNA and control [29].

Mammalian vectors (2 µg) were incubated or co-incubated with siRNA with the cells for 48 h at 37°C. Cx43 clones were as described [29]. Cx43 siRNA insensitive clones (labeled by *) were generated by introducing three nucleotide switches, T1294C, T1297G and A1300G by using P1(+), 5'-ctaaaaaactagccgcggggcatgaattacagccact-3'; P1(-), 5'-agtggctgtaattcatgccccgcggctagttttttag-3'. GFP-Cx43* R370E vector was generated with primers P2(+), 5'-gcagagccagcagtgaagccagcagcagacct-3'; P2(-), 5'-aggtctgctgctggcttcactgctggctctgc-3'. GFP-Cx43* R370E S364A, GFP-Cx43* R370E S365A, GFP-Cx43* R370E S368A, GFP-Cx43* R370E S369A, GFP-Cx43* R370E S372A, GFP-Cx43* R370E S373A, GFP-Cx43* R370E S364D, GFP-Cx43* R370E S365D, GFP-Cx43* R370E S368D, GFP-Cx43* R370E S369D, GFP-Cx43* R370E S372D and GFP-Cx43* R370E S373D were generated

198 by using respectively P3(+), 5'-gaccagcgacctgcaagcagagcc-3'; P3(-), 5'-ggctctgcttgcaggtcgctggtc-3';
199 P4(+), 5'-cagcgaccttcagccagagccagc-3'; P4(-), 5'-gctggctctggctgaaggtcgctg-3'; P5(+), 5'-
200 caagcagagccgccagtgaagccagc-3'; P5(-), 5'-gctggcttcactggcggctctgcttg-3', P6(+), 5'-
201 cagagccagcgctgaagccagc-3'; P6(-), 5'-gctggcttcagcgctggctctg-3', P7(+), 5'-
202 cagtgaagccgccagcagacctcgg-3'; P7(-), 5'-ccgaggtctgctggcggcttcactg- 3', P8(+), 5'-
203 tgaagccagcgccagacctcggc-3'; P8(-), 5'-gccgaggtctggcgctggcttca-3', P9(+), 5'-
204 gaccagcgacctgacagcagagccagt-3'; P9(-), 5'- actggctctgctgtcaggtcgctggtc-3'; P10(+), 5'-
205 cagcgaccttcagacagagccagc-3'; P10(-), 5'- gctggctctgtctgaaggtcgctg-3'; P11(+), 5'-
206 caagcagagccgacagtgaagccagc-3'; P11(-), 5'- gctggcttcactgtcggctctgcttg-3', P12(+), 5'-
207 cagagccagcgatgaagccagc-3'; P12(-), 5'-gctggcttcatcgctggcttcactg-3', P13(+), 5'-
208 cagtgaagccgacagcagacctcgg-3'; P13(-), 5'-ccgaggtctgctgtcggcttcactg-3', P14(+), 5'-
209 tgaagccagcgacagacctcggc-3'; P14(-), 5'-gccgaggtctgtcgctggcttca-3'. Cx43* R370E S369A-S373A was
210 generated using P15(+), 5'-gagccagcgctcgtgccagcgccagacctcggcctgatgacc-3'; P15(-), 5'-
211 ggtcatcaggccgaggtctggcgctggcacgagcgctggctc-3' and Cx43* R370E S369D-S373D were generated by
212 using successively primers P12 and P14 respectively. Sequences corresponding to Cx43* presenting 6
213 serine substitutions in alanine (A) or aspartic acid (D) were purchased from GeneArt (Life
214 Technologies, Illkirch, France). For 6SA; 5'-
215 gaattctaaaaaactagccgcggggcatgaattacagccactagccattgtggaccagcgacctgcagccagagccgccgctcgtgccgccgcc
216 agacctcggcctgatgacctggagatct-3' and for 6SD; 5'-
217 gattctaaaaaactagccgcggggcatgaattacagccactagccattgtggaccagcgacctgacgacagagccgacgaccgtgccgacgaca
218 gacctcggcctgatgacctggagatct-3'. All vectors were cloned into pENTR/D-TOPO vector using the
219 gateway cloning technology (Life Technologies, Illkirch, France) and thereafter transferred into
220 pDEST-EGFP to yield an GFP-Cx43 fusion protein (GFP-tag in N-terminus). All constructs were
221 verified by sequencing.
222
223 **Gap-Fluorescence Loss In Photobleaching (FLIP) experiments**
224 Gap junction communication was quantitatively followed in live cells by gap-FLIP. Briefly, HEK293
225 cells were cultured in IBIDI μ-Slide 8 well (Biovalley, France) and transfected as described above 18

hours prior to observation. The images were acquired on a spinning disk microscope. The Spinning disk microscope is based on a CSU-X1 Yokogawa head mounted on an inverted Ti-E Nikon microscope equipped with a motorized XY Stage. Images were acquired through a 60x 1.4NA Plan-Apo objective with a QuantEM EMCCD camera (Photometrics, USA). Optical sectioning was achieved using a piezo stage (Nano-z series, Mad City Lab, USA). A Roper/ Errol laser bench was equipped with 405, 491 and 561 nm laser diodes, delivering 50 mW each, coupled to the spinning disk head through a single fiber. Multi-dimensional acquisitions were performed in streaming mode using Metamorph 7.7.6 software (Molecular Devices, France). Cells were incubated with 5 µM calcein Red-Orange AM (Thermo Scientific, France) for 5 min at 37°C. Subsequently, cells were placed inside the temperature controlled chamber (temperature and CO_2) of the microscope and imaged for FLIP analysis with a Fluorescence Recovery After Photobleaching (FRAP) head (Errol and Roper, France). A single region (ROI) of a selected target cell (C1) was photobleached on a 9.8 μm^2 area for 300 ms each 10 s with 60 repetitions. Fluorescence loss images were acquired every time points with an attenuated laser beam (0.9 mW from the pupil of the objective). Quantification of the fluorescence loss in C1 and a neighbouring connected cell (C2) was performed by ImageJ software. The intensity of fluorescence was normalized by subtracting noise background, non-specific bleaching and plotted on the graph using GraphPad Prism 6 (La Jolla, USA). Kymograms show the FLIP time course. The mobile fraction was determined as (span/ F_i) x 100, with span as F_i - F_∞, where F_∞ is the fluorescence in C2 after fluorescence loss at infinite time; F_i is the fluorescence in C2 before bleaching. The recovery curves were fit by non-linear regression and the plateau followed by one-phase decay equation using GraphPad Prism 6 (La Jolla, USA). Mobile fractions were obtained by fitting curves with GraphPad Prism 6 (La Jolla, USA).

Statistics

Quantitative data are presented as mean ± SEM. Statistical differences between three or more groups were evaluated using ANOVA test with either Tukey post hoc analaysis when comparing every mean with every other mean or Dunnett's post hoc analysis to compare every mean with a control mean.

Student's unpaired t-test were performed to compare means of two unmatched groups. Means difference were considered significant when $p < 0.05$.

Results

PKA phosphorylates Cx43 and promotes cell fusion

To assess the effect of PKA on trophoblast fusion, primary cultures of CT cells from human placenta were cultured for 48 h in the presence of a cell-penetrating Arg-tagged version of the protein kinase A inhibitor (PKI) peptide or a corresponding scrambled control (scrambled PKI). Subsequently, cell fusion assays were performed by assaying the nuclear distribution in syncytia *versus* mononuclear cells. This was achieved by immunostaining cellular boundaries using a specific marker of the human trophoblast plasma membrane (desmoplakin) together with a nuclear counterstain (DAPI). Mononuclear CTs spontaneously aggregate at 24 h of culture and fuse to form multinucleated syncytia between 48 and 72 h. Trophoblasts incubated with scrambled PKI control underwent normal cell fusion as evident from discontinuous desmoplakin immunostaining, quantified mononuclear aggregated cells, and fusion indices (*i.e.* the percentage of trophoblast nuclei present in multinucleated cells) (Fig. 1A). In contrast, trophoblasts cultured with PKI aggregated but displayed impaired cell fusion. This indicates that spontaneous fusion is PKA-driven. The cell fusion process is accompanied by an increase in secretion of pregnancy hormones (*i.e.* hCG and hPL). Treatment with PKI decreased significantly both hCG and hPL secretion compared to scrambled PKI (Fig. 1A). Together these data suggest that PKA activity plays a role in the regulation of trophoblast fusion.

We next characterized phosphorylation levels of Cx43 in trophoblasts cultured with scrambled PKI or PKI under basal conditions and in the presence of 8-CPT-cAMP to activate PKA. The use of a cell-penetrating form of PKI in human trophoblasts in the absence of a cAMP stimulus displayed similar levels of phosphorylation of Cx43 compared as cells cultured with scrambled PKI (Fig. 1B). As control, we examined the phosphorylation levels of other substrates of PKA as identified by an anti-phospho PKA substrate antibody that recognizes the sequence RRXpS. Here, we noticed a low level of phosphorylation of some PKA-substrates under basal conditions that was reduced in PKI treated cells (Fig. 1B). This is in agreement with earlier studies indicating low tonic levels of cAMP in

primary human trophoblasts sufficient to drive phosphorylation of some PKA substrates [19, 20, 51]. Interestingly, in trophoblasts cultured with 8-CPT-cAMP, PKI reduced the levels of phosphorylated Cx43 (P1 and P2 forms) over unphosphorylated Cx43 by approximately 50% ($p < 0.001$) compared with cells treated with scrambled PKI (Fig. 1B). The total levels of Cx43 and ezrin remained unchanged in cultures treated with either PKI or the corresponding scrambled control. Again, PKI decreased phosphorylation levels also of PKA-substrates in cells cultured with 8-CPT-cAMP (Fig. 1B). Cx43 phosphorylation by kinases is speculated to control gap junction assembly, communication, and recycling [42].

We next investigated the physical vicinity between Cx43 and a cell-membrane marker (desmoplakin) as well as Cx43 and ezrin by proximity ligation assays (PLA) in unstimulated or 8-CPT-cAMP stimulated trophoblasts that were pre-incubated for 24 h with PKI or scrambled PKI. We established by co-immunostaining that Cx43 and desmoplakin co-distribute to the plasmalemma subset of human trophoblasts (Supplementary Fig. S1A). As evident from micrographs and histograms, PKI significantly reduced the proximity of Cx43 to the cell membrane (desmoplakin) in both stimulated and unstimulated cells and compared with the scrambled control ($p < 0.001$ for both; Fig. 1C and Supplementary Fig. S1B). Furthermore, we noticed that stimulation with 8-CPT-cAMP slightly increased the Cx43 protein expression at the cell membrane in both scrambled PKI and PKI treated cells ($p < 0.05$; Fig. 1C). These observations indicate that PKA activity is necessary to promote Cx43 assembly at the cell membrane. Conversely, we observed no significant changes in PLA between Cx43 and ezrin in stimulated or unstimulated cells cultured with or without PKI (Supplementary Fig. S1B).

Ezrin brings PKA in vicinity of Cx43

A complex of the gap junction protein Cx43 and the AKAP ezrin has been shown to play an important role in trophoblast fusion [29]. For this reason, we investigated the possibility of a physical interaction between the PKA regulatory and catalytic subunits and the Cx43-ezrin complex. Immunoprecipitation of ezrin pulled down Cx43, PKA RIα, PKA RIIα and PKA Cα (Fig. 2A). Conversely, immunoprecipitation of Cx43 pulled down ezrin and PKA RIα, RIIα and Cα subunits (Fig. 2A).

Furthermore, immunoprecipitation of PKA Cα or regulatory subunits co-precipitated Cx43 and ezrin. Interestingly, AKAP18, a known AKAP for PKA type II, was not pulled down following ezrin, Cx43 or PKA RIα immunoprecipitations, while PKA RIIα and Cα subunit immunoprecipitations did. These results indicate that in human trophoblasts the PKA holoenzyme is part of a macromolecular complex encompassing ezrin and Cx43 complex.

To examine the colocalization of ezrin, PKA regulatory and catalytic subunits, and Cx43 in trophoblasts, we performed PLA in permeabilized cells with pairs of specific antibodies (Fig. 2B). This demonstrated that PKA Cα and Rα subunits were in close proximity to ezrin and Cx43, as evident from the appearance of white dots (Fig. 2B and normalized in Supplementary Fig. S1C). PLA was negative when either antibody in these pairs was replaced with nonspecific mouse and rabbit IgG primary antibodies.

In line with the observations on proximity by PLA, ezrin, Cx43 or PKA Cα were immunoprecipitated from human trophoblasts and assayed for associated PKA activity with or without PKI (Fig. 1C). As evident from the histograms, PKA activity was associated with ezrin and Cx43 immunoprecipitates ($p < 0.01$ and $p < 0.05$, respectively, and compared to IgG control). Furthermore, PKI significantly reduced the PKA activity in ezrin and Cx43 immunocomplexes ($p < 0.01$ and $p < 0.05$ respectively). This supports the notion that PKA anchored to the signaling complex regulates gap junction communication. As expected, strong PKA activity was observed in PKA Cα subunit immunoprecipitation ($p < 0.05$ compared with IgG control) that was abolished in presence of PKI ($p < 0.05$ compared with control), whereas no activity was co-precipitated with control IgG.

Delineation of PKA phosphorylation residues on Cx43

Phosphorylation of Cx43 in the C-terminal domain regulates gap junction assembly, communication, and recycling. However, PKA-dependent phosphorylation sites on Cx43 and associated functions remain elusive. To address this gap we prepared peptide arrays encompassing amino acids V359 to R376 of the Cx43 C-terminal (Cx43-CT) region, where single or multiple combination of serine substitutions with alanine were included, by synthetizing peptides on solid phase. This region displays 6 serines (S364, S365, S368, S369, S372 and S373) that could putatively be phosphorylated by PKA.

The resulting filters were subjected to phosphorylation with recombinant PKA. The level of PKA phosphorylation for each peptide was next quantified (Fig. 3A-C and Supplementary Fig. S2A-B). Filter analysis revealed that peptides covering the Cx43-CT region were phosphorylated by PKA to varying extents depending on the substitutions incorporated (Fig. 3A-B and Supplementary Fig. S2B). A peptide from the wild type Cx43-CT region (WT) showed a high level of phosphorylation by PKA (blue bar, $p < 0.001$), as did positive controls (peptides with consensus and CREB PKA phosphorylation sites), whereas a negative control, a peptide with the consensus phosphorylation site for CK1D did not (Fig. 3A). Of note, the level of PKA phosphorylation of Cx43 was weaker ($p < 0.001$) than that of the consensus and CREB PKA phosphorylation sites (Fig. 3A).

Phosphorylation of peptides with single amino acid substitutions of serines with alanines reduced levels of PKA phosphorylation for Cx43-S369A and Cx43-S373A ($p < 0.001$, lilac and purple bars) compared with the phosphorylation of the wild type sequence (Fig. 3B, blue bar). Interestingly, no modification in the level of PKA phosphorylation appeared for any other single serine substitution (*i.e.* S364, S365, S368 and S372). This indicates that S369 and/or S373 of Cx43-CT region are preferentially phosphorylated by PKA. To explore this further, we next investigated combinations of serine substitutions (Fig. 3C and Supplementary Fig. S2A-B). The random combination of double serine substitution of S364, S365, S368 or S372 residues showed no significant reduction in PKA-dependent phosphorylation compared with the level of phosphorylation of a peptide covering the WT Cx43-CT region (Fig. 3C). However, the double substitution of S369A and S373A reduced PKA-dependent Cx43-CT phosphorylation by > 50% ($p < 0.001$, green bar) compared with the phosphorylation of the wild type sequence (Fig. 3C, blue bar). Interestingly, the level of PKA phosphorylation on the Cx43 S369-373A sequence was not found to be significantly different from the level of PKA phosphorylation of the negative control that is not phosphorylated by PKA (*i.e.* the consensus CK1D phosphorylation site). A similar reduction in PKA phosphorylation was observed with four or five serine substitutions in the Cx43-CT sequence that included substitution of S369 and S373 (Supplementary Fig. S2B). Jointly, these observations support the notion that S369 together with S373 are the major PKA phosphorylation sites in the Cx43-CT domain when examined *in vitro*.

NanoLC-LTQ Orbitrap mass spectrometry (MS) analysis was next performed to identify the residues in Cx43 that are phosphorylated *in vivo* as a consequence of activation of the cAMP signaling pathway. To minimize sample variability and to increase sample concentration required for MS analysis, IAR20, a liver epithelial cell line with abundant Cx43, was used for these analyses. IAR20 cells were cultured with or without 8-CPT-cAMP and cell lysates were subjected to Cx43 immunoprecipitation. Excised bands from SDS-PAGE of immunoprecipitates were subjected to tryptic digestion and analyzed by MS (Fig. 3D-E). This approach identified ezrin, PKA RIα, PKA RIIα, PKA Cα, and Cx43 in the Cx43 immunoprecipitates (Fig. 3D). This supports the earlier finding of ezrin and Cx43 forming a signaling complex with PKA also in other cell types than placental trophoblasts. The analysis of individual Cx43-CT peptides from parallel immunoprecipitates further revealed the presence of a mix of peptides that were phosphorylated or unphosphorylated on S364, S365, S368 and S369 in Cx43 immunoprecipitates from untreated IAR20 cells (Fig. 3E and Supplementary Fig. S3A). As expected, similar phospho-peptides were also found in Cx43 immunoprecipitates from IAR20 cells treated with 8-CPT-cAMP. However, in addition we identified new phospho-peptides that were phosphorylated on S372 and S373 in the treated cells (Fig. 3E and Supplementary Fig. S3B). Together the data from peptide arrays and MS analysis verify that S369 and S373 are phosphorylated by PKA in the C-terminal region of Cx43, and that particularly S373 is phosphorylated upon acute activation of the cAMP signaling pathway.

Subcellular distribution of phospho-mimetic forms of Cx43

Cx43 phosphorylation triggers gap junction assembly or recycling and subsequent subcellular relocalization. To examine the plasma membrane localization of the different phosphorylated variants of Cx43, trophoblasts were transfected with green fluorescent protein (GFP)-tagged phosphomimetic forms of Cx43 followed by PLA analysis with a pair of specific antibodies against desmoplakin and GFP (Fig. 4A and Supplementary Fig. S4A). To avoid interference by endogenous PKA phosphorylation we employed mammalian expression vectors encoding Cx43 with a substitution that abolishes ezrin binding and thereby detaches PKA from the complex (R370E; [29]) fused to GFP (GFP-Cx43). We next introduced phosphomimetic (S/D) and phosphomutant (S/A) substitutions at

serine residues 364, 365, 368, 369, 372 and 373. GFP-Cx43 R370E was expressed at the plasma membrane in human trophoblast and colocalized with desmoplakin as evident from the appearance of magenta dots ($p < 0.001$), whereas GFP control did not (Fig. 4B). Interestingly, the level of colocalization with desmoplakin remained the same for most of the GFP-Cx43 R370E phosphomimetic or phosphomutant forms (364, 365, 368 and 372) compared with GFP-Cx43 R370E. We noticed an exception for GFP-Cx43 R370E+S369D and GFP-Cx43 R370E+S373D, which displayed significant increases in plasma membrane localization compared with GFP-Cx43 R370E ($p < 0.01$ and $p < 0.05$ respectively). Furthermore, pairwise comparison of colocalization between corresponding phosphomimic and phosphomutant Cx43 forms revealed that aspartate substitution at S365, S369, S372 or S373 significantly increased the desmoplakin-colocalization at the plasma membrane compared to the respective alanine-substituted phosphomutant form ($p < 0.05$, 0.01, 0.05 and 0.01 respectively). Surprisingly, phosphomimic and phosphomutant substitutions at position S364 or S368 did not alter the localization at the plasma membrane of these Cx43 constructs in human trophoblasts. It is noteworthy that expression of constructs with the 6 serine phospho-sites replaced with aspartate (6SD) or the double S369-373D mutant increased Cx43 colocalization at the plasma membrane ($p < 0.001$ and $p < 0.05$, respectively) compared with GFP-Cx43 R370E control, whereas the corresponding phosphomutant variants with alanine substitutions (6SA and S369-373A) displayed significantly less expression at the membrane ($p < 0.001$ for both). Together, these data suggest that the phosphorylation on S369 and/or S373 promotes assembly of Cx43 at the plasma membrane of human trophoblasts.

Phospho-mimetic forms of Cx43 trigger human trophoblast fusion

PKA and Cx43 gap junction communication trigger human trophoblast fusion [12, 20, 29]. The present data suggest that S369 and S373 of the Cx43-CT domain are the major residues phosphorylated by PKA. We analyzed the functional consequences of alterations of residues S364 (described previously to be phosphorylated by PKA; [52]), S369, and S373 in fusion of primary human trophoblasts. Human trophoblasts were transfected with Cx43-specific siRNA or

corresponding scrambled control and incubated for 48 h. siRNA-mediated knockdown of Cx43 reduced protein expression compared with cells transfected with scrambled siRNA (70% reduction; $p < 0.001$; Supplementary Fig. S4B and Fig. 5A). Human trophoblasts with Cx43 knockdown displayed cellular aggregation associated with a decrease in cell fusion by approximately 65% ($p < 0.001$) compared with fusion of trophoblasts transfected with scrambled control (Fig. 5B-C). In addition to this defect in morphological differentiation upon knockdown of Cx43, we observed a decrease in the functional differentiation of the trophoblast with a significant reduction in secretion of syncytial hormones (hCG and hPL) ($p < 0.001$ for both; Fig. 5D). This is supported by correlation studies in which a weak fusion index is associated with low syncytial hormone secretions (Supplementary Fig. S4C. Pearson's R coefficient of 0.82 and 0.85 for hCG and hPL respectively; $p < 0.001$ for both). Next, we employed a combined strategy of RNA interference and reconstitution experiments with various phosphomimic or phosphomutant forms of Cx43. Primary human trophoblasts were depleted of endogenous Cx43 by siRNA transfection. Simultaneously, we transfected cells with mammalian expression vectors encoding siRNA-resistant wild-type Cx43 or Cx43 R370E fused to GFP (GFP-Cx43* and GFP-Cx43* R370E, respectively), with or without phosphomimic or phosphomutant substitutions in the indicated phosphorylation sites (all six, single or double serine substitutions) that formed complexes with the expected composition (Supplementary Fig. S5A). As evident from discontinuous desmoplakin immunostaining, fusion indices and hormone secretion, cells reconstituted with GFP-Cx43* after knockdown of endogenous Cx43 formed syncytia (Fig. 5B-D). By contrast, trophoblasts reconstituted with GFP-Cx43* R370E that does not bind ezrin and therefore does not target PKA to the Cx43 complex, aggregated but did not fuse (Fig. 5B-C). This defect in trophoblast fusion was associated with decreased syncytial hormone production compared with cells treated with scrambled control (Fig. 5D and Supplementary Fig. S4C; $p < 0.05$ for hCG and $p < 0.001$ for hPL). Trophoblasts with knockdown of endogenous Cx43 reconstituted with GFP-Cx43* R370E with alanine substitutions individually mimicking phospho-resistant residues at position 364, 369 and 373 (GFP-Cx43* R370E S364A, GFP-Cx43* R370E S369A or GFP-Cx43* R370E S373A), in position 369 and 373 combined, or at all 6 positions displayed aggregated but unfused cells as evident from low fusion indices (Fig. 5B-C). These reductions in cell fusion were associated with significant

decreases in hCG and hPL secretion (Fig. 5D and Supplementary Fig. S4C). By contrast, cells reconstituted with GFP-Cx43* R370E, in which corresponding serines were replaced with aspartate substitutions to mimic a phosphorylated state, (GFP-Cx43* R370E+S364D, GFP-Cx43* R370E+S369D, GFP-Cx43* R370E+S373D, GFP-Cx43* R370E+6SD, or GFP-Cx43* R370E+S369-373D) formed syncytia (Fig. 5B-C). Correlation analysis suggests that reconstitution of trophoblast cell fusion was also associated with reconstitution of syncytial hormone secretion (Fig. 5D and Supplementary Fig. S4C). Interestingly, cells reconstituted with constructs expressing GFP-Cx43* variants that rescued syncytial formation and hormonal secretion (*i.e.* GFP-Cx43* and constructs with aspartate substitution: GFP-Cx43* R370E+S369D, GFP-Cx43* R370E+S373D), cultured with PKI showed a reduction in hCG secretion compared with cells treated with scrambled PKI (Fig. 5E). However, trophoblasts reconstituted with GFP-Cx43* R370E with or without alanine substitution and cultured with PKI or corresponding scrambled control exhibited a similar low rate of hCG secretion, which is consistent with data presented in figure 5B-D. In addition, HEK293 cells reconstituted with constructs expressing GFP-Cx43* and cultured with 8-CPT-cAMP showed an increased level of phosphorylated GFP-Cx43 at serine 373 that was inhibited with PKI (Supplementary figure S4D). In contrast, cells reconstituted with GFP-Cx43* with alanine substitutions in position 369 and 373 combined (GFP-CX43* S369-373A) did not display this regulation of cAMP-dependent phosphorylation (Supplementary figure S4D). Taken together, the results of these knockdown and rescue experiments suggest that phosphorylation of specific residues (S369 and S373) in Cx43-CT domain can be targeted by PKA and trigger trophoblast cell fusion and syncytial hormone production.

S369 and S373 phospho-mimetic variants of Cx43 trigger gap junction communication

We next characterized functional consequences of phosphomimic and phosphomutant substitutions in the Cx43-CT domain on gap junction communication. Gap-FLIP (Fluorescence Loss In Photobleaching) analyses were performed on HEK293 cells transfected with GFP-control or GFP-Cx43* or GFP-Cx43* R370E, with or without phosphomimic and phosphomutant substitutions at the

indicated phosphorylation sites (all six, single, or double serine substitutions). Cells were loaded with calcein-AM dye and pairs of transfected cells were chosen for FLIP analysis (Fig. 6). Simultaneously, the targeted-cell (C1) was repetitively bleached while the calcein fluorescence intensity of the adjacent cell (C2) was monitored over the time (Fig. 6A). Kymograms (displaying the temporal evolution of the fluorescent intensity) together with high-magnification views and fluorescence intensity curves (Fig. 6A) indicated that the fluorescence loss of C2 is linked to repeated light beam exposure on C1 and thus reflects the gap junction communication between pairs of cells. HEK293 cells used in the present study expressed a very low level of endogenous Cx43 (Supplementary Fig. S5B) and displayed a correspondingly low gap junction communication as evident from fluorescence intensity curves of GFP-control transfected cells (Fig. 6A) and the associated mobile fraction (Fig. 6B). Interestingly, expression of GFP-Cx43* increased gap junction communication compared to GFP-control transfected cells (above 50% increase in mobile fraction, $p < 0.001$). Conversely, cells transfected with GFP-Cx43* R370E showed a similar profile of gap junction communication as GFP-control transfected cells. This is consistent with our model that ezrin associated with Cx43 is involved in the PKA-mediated modulation of gap junction communication. Cells transfected with GFP-Cx43* R370E with aspartate substitutions mimicking phosphorylated residues at positions 364, 369, and 373 individually or combined at positions 369 and 373, or in all 6 phosphosites of the Cx43-CT domain, displayed an increase in the mobile fraction of dye and thus in gap junction communication compared to GFP-control or GFP-Cx43* R370E transfected cells (Fig. 6B and supplementary Fig. S5C; above 50%, $p < 0.001$ for all). Conversely, substitutions mimicking dephosphorylation in the Cx43-CT domain exhibited a significantly decreased gap junction communication compared to the corresponding phospho-mimetic substitutions (Fig. 6B and supplementary Fig. S5C; $p < 0.001$ for all except for double substitution in S369-373 $p < 0.01$). Together, these experiments indicate that PKA-dependent phosphorylation of S369 and S373 of Cx43-CT domain promotes gap junction communication and furthermore that this effect depends on PKA anchoring by ezrin.

Discussion

The present study reports that ezrin binds the Cx43 carboxyterminal domain and recruits PKA to directly or indirectly facilitate phosphorylation of Cx43 on serines 369 and 373, which promotes gap junction assembly at the plasma membrane of human trophoblasts, triggers gap junction communication and thereby cell fusion. Our study is consistent with the conclusions of an earlier report by TenBroek et al. [52], where the authors concluded that the carboxyterminal of Cx43 is critical for mediating effects of cAMP, possibly by facilitating interactions with trafficking proteins to enhance GJ assembly. The site of such interactions was suggested to reside in the region of S364 and that the phosphorylation of this site appeared to be necessary for effects of cAMP on assembly that follows.

Human primary trophoblasts undergo cell fusion both *in vivo* and in culture to form an endocrinologically active syncytium; a differentiation process that is driven by hCG acting through the cAMP signaling pathway, and that in culture also proceeds spontaneously, albeit slower [20, 53]). In primary human trophoblasts we found that a specific inhibitor of the PKA catalytic subunit (*i.e.* PKI) reduced the production of hCG reflecting the reduction in trophoblast fusion. Interestingly, we noticed that these effects are associated with decreased Cx43 phosphorylation and gap junction assembly, suggesting that human CTs have a basal level of cAMP production and tonic PKA activation. This is in agreement with previous observations and compatible with the spontaneous fusion in culture due to auto- or paracrine effects of hCG [19, 20, 51]. Furthermore, addition of a cAMP analog, also known to potentiate human trophoblast fusion, increased Cx43 gap junction assembly, a process that is inhibited in the presence of PKI and that supports a role for PKA activity being involved in Cx43 gap junction assembly. Such regulation has also been reported in other cell models as reviewed in [54]. By co-immunoprecipitation, proximity ligation assays, and mass spectrometry we show that PKA regulatory and catalytic subunits located in a supramolecular complex that includes ezrin and Cx43, in agreement with our previous observations [29]. In this study we characterized the physiological role of this signaling complex further and showed by immunoprecipitation of ezrin and Cx43 that PKA activity was associated with the complex and that treatment with PKI reduced the level of Cx43 phosphorylation in human trophoblasts. Moreover, we demonstrate that silencing Cx43 expression

decreased gap junction communication, syncytial formation, and associated hormonal production, which were reconstituted upon expression of a Cx43 siRNA-insensitive construct. These findings support a central role for Cx43 in trophoblast fusion in agreement with our previous observations [12, 29]. However, reconstitution with a mutant Cx43 R370E with impaired ability to bind ezrin did not restore trophoblast fusion, highlighting the critical role of ezrin to trigger gap junction communication, cell fusion and functional differentiation of human trophoblasts. This led us to propose that the pool of PKA anchored to ezrin coordinates Cx43 phosphorylation, which induces trophoblast fusion. Although Cx43 has been shown to be a poor substrate for PKA compared to other kinases, anchoring of PKA *via* the AKAP ezrin bound to the substrate reduces the degrees of freedom and facilitates phosphorylation. This agrees with earlier observations showing that activation of the cAMP signaling pathway increases Cx43 phosphorylation, gap junction assembly and communication [44, 52, 55, 56]. However, identification of the phosphorylated residues in Cx43 has remained controversial and the associated functional consequences have not been fully elucidated [43-45, 57]. PKA phosphorylation sites are located in the C-terminal part of the protein (Cx43-CT) [54]. This region encompasses amino acids 359 to 376 and harbors repetitions of R-X-X-S/T, the described consensus PKA phosphorylation motif [58, 59].

To further investigate the presumed PKA phosphorylation sites in Cx43, we performed *in vitro* phosphorylation experiments with an array of peptides covering the region. Unexpectedly, we neither found serine 364 to be effectively phosphorylated by PKA *in vitro* nor that activation of PKA promoted phosphorylation of S364 in cells. It is noteworthy that S364 of Cx43 has earlier been described as the main target for cAMP signaling and PKA, the phosphorylation of which promotes gap junction assembly and communication [52, 60, 61]. In the cell types examined here S364 was constitutively phosphorylated in resting cells under basal conditions without induction of cAMP signaling. This has also been noted by others [52, 60]. We cannot exclude the possibility that low levels of PKA activity could constitutively phosphorylate S364 in resting cells, or that PKA or alternate cAMP effector molecules could activate another kinase that phosphorylates S364 through a crosstalk mechanism. Shah and colleagues have shown that a peptide sequence encompassing amino acids 359 to 376 of Cx43-CT domain, in which S364 was replaced with proline displayed 50% less

PKA-dependent phosphorylation, and thus proposed S364 to serve as the main PKA target in Cx43 [60]. However, this observation revealed that other residues in this sequence were also phosphorylated. Here we propose serines 369 and 373 as the principal PKA targets. Discrepancies regarding S364 may be attributable to differences of 3D folding of the intact protein as studied by Shah et al., *versus* the peptide array used here as spatial organization may affect PKA phosphorylation at this site. Furthermore, our gap-FLIP experiments and fusion assays demonstrated that phospho-mimicking substitutions in residue 364 of Cx43-CT domain promoted intercellular communication, which triggered trophoblast differentiation with an increase in cell fusion and syncytial hormone production. These observations are in agreement with previous studies [12, 29] and support the possibility that S364 could be a phosphorylation target that regulates Cx43 function. Although we speculate that this residue is not directly phosphorylated by PKA, our data indicate that its phosphorylation would facilitate opening of the Cx43 channel and thus might be involved in the first steps of trophoblast fusion, *e.g.* prior to the activation of cAMP signaling and could act in concert with other cAMP-regulated phosphorylation sites (*i.e.,* S369 and S373) to accelerate cell communication and cell fusion in later stages of placental differentiation.

The present MS analysis found S365 to be phosphorylated under basal conditions and the PLA experiments suggested that mimicking phosphorylation at this position also promotes Cx43 gap junction assembly. These observations are in agreement with a previous study in which S365 phosphorylation was reported to serve as a gatekeeper to prevent down-regulation of Cx43 by PKC-mediated phosphorylation of S368 [62]. Furthermore, PLA experiments showed that expression of a construct mimicking phosphorylation at S368 reduced gap junction assembly, further supporting this role for PKC [63]. In contrast, expression of a Cx43 variant mimicking phosphorylation of S372, a site described to be targeted by PKC *in vitro* [64], promoted gap junction assembly. Further experiments are needed to decipher kinetic and the functional consequences of PKC phosphorylation on these residues.

The *in vitro* phosphorylation assays indicated that serines 369 and 373 are the residues in the Cx43-CT region favored by PKA. This finding is supported by a previous study that proposed that phosphorylation of these residues in granulosa cells cultured with FSH (follicle-stimulating hormone)

583 [65]. FSH signals mainly, but not only, through production of intracellular cAMP and the authors
584 suggested that these residues are phosphorylated in response to the cAMP signaling. We demonstrated
585 that constructs directing expression of Cx43 with phosphomimicking substitutions at positions 369
586 and/or 373 exhibited increase cell membrane expression, supporting an increase in gap junction
587 assembly, which was as reported [60, 64, 66-69]. The present silencing and reconstitution experiments
588 together with gap-FLIP studies using various Cx43 mutants containing phosphoresistant substitutions
589 at S369 and/or S373 indicated that the loss of PKA-specific phosphorylation in the Cx43-CT domain
590 impaired gap junction communication, cell fusion, and thus production of specific pregnancy
591 hormones. Conversely, overexpression or reconstitution with the corresponding phosphomimetic
592 forms restored gap junction communication, trophoblast fusion, and syncytial functions, thus
593 validating the significance of S369 and S373 phosphorylation. Interestingly, reconstitution
594 experiments with phosphomimicking substitutions at positions 369 or 373 and cultured with PKI did
595 not restore production of specific pregnancy hormones. This is consistent with previous observations
596 that highlight the PKA-signaling activation as a pre-requisite for trophoblast fusion [16]. Of note,
597 PKA leads on one hand to phosphorylation and an increase in specific gene expression of fusogenic
598 proteins (*e.g.* syncytins and cadherin) and on the other hand to hCG secretion that acts in a auto- or
599 paracrine manner to initiate and maintain the fusion process (for review see 16). Thus, the use of PKI
600 blocked PKA signaling, which prevents triggering of trophoblast fusion upstream of the step that
601 requires the Cx43 PKA-dependent phosphorylation and the transfer of fusogenic signal through gap
602 junctions. Hence, Cx43 phosphorylation on S369 and/or S373 by anchored-PKA through ezrin is
603 necessary but insufficient to promote alone trophoblast fusion without the concomitant PKA activation
604 in basal or in hCG-stimulated cells.

605 Mass spectrometry and immunoblots revealed S373 not to be phosphorylated under basal
606 conditions but phosphorylated in cells upon acute cAMP stimulation, while S369 was constitutively
607 phosphorylated. As with S364, we speculate that phosphorylation of S369 can occur by low tonic
608 PKA activity or be induced by other kinases. In the line with this suggestion, residues 369 and 373
609 have been linked to Akt/PKB phosphorylation [66, 68, 70]. The Akt consensus phosphorylation
610 sequence R-X-R-X-X-S/T [71] overlaps with that of PKA and the two kinases share phosphorylation

611 sites in various biological contexts [72, 73]). Our data agree with previous studies in which
612 phosphorylation of S373 by Akt induces gap junction assembly and communication [68, 69]. We
613 propose that PKA and Akt signaling work in concert to phosphorylate similar residues in Cx43-CT to
614 preserve a fundamental mechanism for coordinated regulation of gap junction functions in response to
615 distinct extracellular stimuli. Interestingly, single or double phopho-mimetic forms of S369 and S373
616 displayed similar Cx43 behavior. This may indicate a redundancy effect to ensure phosphorylation by
617 PKA in order to trigger a proper associated biological effect (*i.e.* cell communication and cell fusion)
618 and/or that these phospho-sites could have a synergistic effect on the level of gap junction
619 communication or selectivity of the channel for the transfer of small molecules. We propose that
620 phosphorylation of S369 occurs upon basal PKA activation or through activation of another kinase
621 (*i.e.* Akt), while, upon acute cAMP stimulation S373 phosphorylation appears to ensure gap junction
622 assembly and intercellular communication necessary to allow trophoblast fusion.

623 Biological effects observed when using the Cx43 mutant with all six serines substituted with
624 alanine or aspartic acid are more difficult to interpret due to the greater effects that six substitutions
625 presumably would have on this structurally disordered C-terminal region of Cx43 [45].

626 Alteration of syncytial formation and regeneration during pregnancy affects fetal growth and
627 outcomes of the pregnancy. Anomalies of villous trophoblast differentiation and cell fusion lead to
628 severe placental abnormalities (*i.e*. intrauterine growth restriction (IUGR) and preeclampsia) [74 , 75].
629 It is noteworthy that cAMP signaling is markedly reduced in placentas from patients with
630 preeclampsia [76]. Furthermore, it has been observed that Cx43 gap junction functions fail in
631 preeclampsia [77]. Together, these observations lead us to speculate that diminished cAMP signaling
632 reduces PKA activation and phosphorylation of the C-terminal domain of Cx43 in preeclampsia.
633 Analysis of the level of Cx43-CT phosphorylation and more precisely that of residues S369 and S373
634 in preeclampsia are needed to better understand the pathology. This could help advance therapies
635 targeting phosphorylation of PKA-specific residues in Cx43-CT to counteract the defect in gap
636 junction communication and cAMP signaling observed in preeclampsia.

637 In summary, using a physiological primary culture model of human trophoblasts, we propose
638 that ezrin binds directly to Cx43 gap junctions and directs PKA to the vicinity of Cx43. This proximity

allows for efficient and rapid phosphorylation of serine 369 and/or 373 in the C-terminal region of Cx43, which promotes gap junction assembly and communication, thereby controlling cAMP-regulated cell fusion.

Acknowledgements

We are grateful to Jorun Solheim, Fatima Ferreira and Camille Fraichard for technical assistance, to Ola Blingsmo for peptide synthesis, to members of the Taskén laboratory for assistance. This work has benefitted from the expertise of Vincent Fraisier (PICT-IBiSA @CNRS-Institut Curie; member of the French National Research Infrastructure France-BioImaging ANR-10-INSB-04) with imaging and RSI professions libérales provinces (44-boulevard de la bastille 75578 Paris Cedex 12). We are grateful to Dr. Peter A. Friedman, University of Pittsburg for critically reviewing and commenting on the manuscript.

Declarations of interest

The authors declare that they have no conflict of interest.

Funding information

This work was supported by the Norwegian Cancer Society, the Research Council of Norway, the Novo Nordic Foundation and the K.G. Jebsen Foundation (to KT), the French institute for medical research (INSERM, to GP and PG) and RSI professions libérales provinces (44-Bd de la bastille 75578 Paris Cedex 12 to GP).

Author contribution statement

GP and KT designed the research; AD, PG, GP, and KT did the experiments and analyzed data; BT did MS-analyses and interpreted the MS-data. GP and KT wrote the paper together with AD. All authors read and commented on draft versions of the manuscript and approved the final version.

665 **References**

666 1 Midgley, A., Pierce, G., Denau, G. and Gosling, J. (1963) Morphogenesis of
667 syncytiotrophoblast in vivo: an autoradiographic demonstration. Science. **141**, 350-351

668 2 Zambonin Zallone, A., Teti, A. and Primavera, M. (1984) Monocytes from circulating blood
669 fuse in vitro with purified osteoclasts in primary culture. J Cell Sci. **66**, 335-342

670 3 Wakelam, M. (1985) The fusion of myoblasts. Biochem J. **15**, 1-12

671 4 Oren-Suissa, M. and Podbilewicz, B. (2007) Cell fusion during development. Trends Cell
672 Biol. **17**, 537-546

673 5 Lu, X. and Kang, Y. (2009) Cell fusion as a hidden force in tumor progression. Cancer Res.
674 **69**, 8536-8539

675 6 Benirschke, K. and Kaufmann, P. (2000) Pathology of the human placenta. Springer-Verlag,
676 New-York.

677 7 Eaton, B. and Contractor, S. (1993) In vitro assessment of trophoblast receptors and placental
678 transport mechanisms. In The human placenta (Redman, C. W., Sargent, I. L. and Starkey, P. M.,
679 eds.). pp. 471-503, Blackwell Scientific Publication, London

680 8 Ogren, L. and Talamentes, F. (1994) The placenta as an endocrine organ: polypeptides. In
681 Physiology of reproduction (Knobil, E. and Neill, J., eds.). pp. 875-945, Raven Press, New-York

682 9 Kliman, H., Nestler, J., Sermasi, E., Sanger, J. and Strauss III, J. (1986) Purification,
683 characterization , and *in vitro* differenciation of cytotrophoblasts from human term placentae.
684 Endocrinology. **118**, 1567-1582

685 10 Pidoux, G., Gerbaud, P., Gnidehou, S., Grynberg, M., Geneau, G., Guibourdenche, J., Carette,
686 D., Cronier, L., Evain-Brion, D., Malassine, A. and Frendo, J. L. (2010) ZO-1 is involved in
687 trophoblastic cell differentiation in human placenta. Am J Physiol Cell Physiol. **298**, C1517-1526

688 11 Coutifaris, C., Kao, L. C., Sehdev, H. M., Chin, U., Babalola, G. O., Blaschuk, O. W. and
689 Strauss, J. F., 3rd. (1991) E-cadherin expression during the differentiation of human trophoblasts.
690 Development. **113**, 767-777

691 12 Frendo, J. L., Cronier, L., Bertin, G., Guibourdenche, J., Vidaud, M., Evain-Brion, D. and
692 Malassine, A. (2003) Involvement of connexin 43 in human trophoblast cell fusion and differentiation.
693 J Cell Sci. **116**, 3413-3421

694 13 Bjerregaard, B., Talts, J. F. and Larsson, L. I. (2011) The endogenous envelope protein
695 syncytin is involved in myoblast fusion. In Cell Fusions: regulation and control (Larsson, L. I., ed.).
696 pp. 267-275, Springer

697 14 Frendo, J. L., Olivier, D., Cheynet, V., Blond, J. L., Bouton, O., Vidaud, M., Rabreau, M.,
698 Evain-Brion, D. and Mallet, F. (2003) Direct involvement of HERV-W Env glycoprotein in human
699 trophoblast cell fusion and differentiation. Mol Cell Biol. **23**, 3566-3574

700 15 Soe, K., Andersen, T. L., Hobolt-Pedersen, A. S., Bjerregaard, B., Larsson, L. I. and Delaisse,
701 J. M. (2011) Involvement of human endogenous retroviral syncytin-1 in human osteoclast fusion.
702 Bone. **48**, 837-846

703 16 Gerbaud, P. and Pidoux, G. (2015) Review: An overview of molecular events occurring in
704 human trophoblast fusion. Placenta. **36 Suppl 1**, S35-42

17 Knerr, I., Schubert, S. W., Wich, C., Amann, K., Aigner, T., Vogler, T., Jung, R., Dotsch, J., Rascher, W. and Hashemolhosseini, S. (2005) Stimulation of GCMa and syncytin via cAMP mediated PKA signaling in human trophoblastic cells under normoxic and hypoxic conditions. FEBS Lett. **579**, 3991-3998

18 Dunk, C. E., Gellhaus, A., Drewlo, S., Baczyk, D., Potgens, A. J., Winterhager, E., Kingdom, J. C. and Lye, S. J. (2012) The molecular role of connexin 43 in human trophoblast cell fusion. Biol Reprod. **86**, 115

19 Pidoux, G., Gerbaud, P., Tsatsaris, V., Marpeau, O., Ferreira, F., Meduri, G., Guibourdenche, J., Badet, J., Evain-Brion, D. and Frendo, J. L. (2007) Biochemical characterization and modulation of LH/CG-receptor during human trophoblast differentiation. J Cell Physiol. **212**, 26-35

20 Keryer, G., Alsat, E., Tasken, K. and Evain-Brion, D. (1998) Cyclic AMP-dependent protein kinases and human trophoblast cell differentiation in vitro. J Cell Sci. **111 (Pt 7)**, 995-1004

21 Pidoux, G. and Tasken, K. (2010) Specificity and spatial dynamics of PKA signaling organized by A kinase anchoring proteins. J Mol Endocrinol. **44**, 271-284

22 Tasken, K. and Aandahl, E. M. (2004) Localized effects of cAMP mediated by distinct routes of protein kinase A. Physiol Rev. **84**, 137-167

23 Carr, D. W., Hausken, Z. E., Fraser, I. D., Stofko-Hahn, R. E. and Scott, J. D. (1992) Association of the type II cAMP-dependent protein kinase with a human thyroid RII-anchoring protein. Cloning and characterization of the RII-binding domain. J Biol Chem. **267**, 13376-13382

24 Gold, M. G., Lygren, B., Dokurno, P., Hoshi, N., McConnachie, G., Tasken, K., Carlson, C. R., Scott, J. D. and Barford, D. (2006) Molecular basis of AKAP specificity for PKA regulatory subunits. Mol Cell. **24**, 383-395

25 Calejo, A. I. and Tasken, K. (2015) Targeting protein-protein interactions in complexes organized by A kinase anchoring proteins. Front Pharmacol. **6**, 192

26 Coghlan, V. M., Perrino, B. A., Howard, M., Langeberg, L. K., Hicks, J. B., Gallatin, W. M. and Scott, J. D. (1995) Association of protein kinase A and protein phosphatase 2B with a common anchoring protein. Science. **267**, 108-111

27 Dodge, K. L., Khouangsathiene, S., Kapiloff, M. S., Mouton, R., Hill, E. V., Houslay, M. D., Langeberg, L. K. and Scott, J. D. (2001) mAKAP assembles a protein kinase A/PDE4 phosphodiesterase cAMP signaling module. Embo J. **20**, 1921-1930

28 Weedon-Fekjaer, M. S. and Tasken, K. (2012) Review: Spatiotemporal dynamics of hCG/cAMP signaling and regulation of placental function. Placenta. **33 Suppl**, S87-91

29 Pidoux, G., Gerbaud, P., Dompierre, J., Lygren, B., Solstad, T., Evain-Brion, D. and Tasken, K. (2014) A PKA-ezrin-connexin 43 signaling complex controls gap junction communication and thereby trophoblast cell fusion. J Cell Sci. **127**, 4172-4185

30 Gerbaud, P., Tasken, K. and Pidoux, G. (2015) Spatiotemporal regulation of cAMP signaling controls the human trophoblast fusion. Front Pharmacol. **6**, 202

31 Pidoux, G. and Tasken, K. (2015) Anchored PKA as a gatekeeper for gap junctions. Commun Integr Biol. **8**, e1057361

744 32 Reczek, D., Berryman, M. and Bretscher, A. (1997) Identification of EBP50: A PDZ-
745 containing phosphoprotein that associates with members of the ezrin-radixin-moesin family. J Cell
746 Biol. **139**, 169-179

747 33 Carlson, C. R., Lygren, B., Berge, T., Hoshi, N., Wong, W., Tasken, K. and Scott, J. D. (2006)
748 Delineation of type I protein kinase A-selective signaling events using an RI anchoring disruptor. J
749 Biol Chem. **281**, 21535-21545

750 34 Ruppelt, A., Mosenden, R., Gronholm, M., Aandahl, E. M., Tobin, D., Carlson, C. R.,
751 Abrahamsen, H., Herberg, F. W., Carpen, O. and Tasken, K. (2007) Inhibition of T cell activation by
752 cyclic adenosine 5'-monophosphate requires lipid raft targeting of protein kinase A type I by the A-
753 kinase anchoring protein ezrin. J Immunol. **179**, 5159-5168

754 35 Jarnaess, E., Ruppelt, A., Stokka, A. J., Lygren, B., Scott, J. D. and Tasken, K. (2008) Dual
755 specificity A-kinase anchoring proteins (AKAPs) contain an additional binding region that enhances
756 targeting of protein kinase A type I. J Biol Chem. **283**, 33708-33718

757 36 Sanderson, M. J., Charles, A. C., Boitano, S. and Dirksen, E. R. (1994) Mechanisms and
758 function of intercellular calcium signaling. Molecular and cellular endocrinology. **98**, 173-187

759 37 Goodenough, D. A., Goliger, J. A. and Paul, D. L. (1996) Connexins, connexons, and
760 intercellular communication. Annu Rev Biochem. **65**, 475-502

761 38 Willecke, K., Eiberger, J., Degen, J., Eckardt, D., Romualdi, A., Guldenagel, M., Deutsch, U.
762 and Sohl, G. (2002) Structural and functional diversity of connexin genes in the mouse and human
763 genome. Biol Chem. **383**, 725-737

764 39 Kumar, N. and Gilula, N. (1996) The gap junction communication channel. Cell. **84**, 381-388.

765 40 Saez, J. C., Berthoud, V. M., Moreno, A. P. and Spray, D. C. (1993) Gap junctions.
766 Multiplicity of controls in differentiated and undifferentiated cells and possible functional
767 implications. Adv Second Messenger Phosphoprotein Res. **27**, 163-198

768 41 Bruzzone, R., White, T. W. and Paul, D. L. (1996) Connections with connexins: the molecular
769 basis of direct intercellular signaling. Eur J Biochem. **238**, 1-27

770 42 Solan, J. L. and Lampe, P. D. (2009) Connexin43 phosphorylation: structural changes and
771 biological effects. Biochem J. **419**, 261-272

772 43 Solan, J. L. and Lampe, P. D. (2017) Spatio-temporal regulation of connexin43
773 phosphorylation and gap junction dynamics. Biochim Biophys Acta

774 44 Lampe, P. D. and Lau, A. F. (2004) The effects of connexin phosphorylation on gap junctional
775 communication. The international journal of biochemistry & cell biology. **36**, 1171-1186

776 45 Grosely, R., Kopanic, J. L., Nabors, S., Kieken, F., Spagnol, G., Al-Mugotir, M., Zach, S. and
777 Sorgen, P. L. (2013) Effects of phosphorylation on the structure and backbone dynamics of the
778 intrinsically disordered connexin43 C-terminal domain. J Biol Chem. **288**, 24857-24870

779 46 Pidoux, G., Witczak, O., Jarnaess, E., Myrvold, L., Urlaub, H., Stokka, A. J., Kuntziger, T.
780 and Tasken, K. (2011) Optic atrophy 1 is an A-kinase anchoring protein on lipid droplets that mediates
781 adrenergic control of lipolysis. EMBO J. **30**, 4371-4386

782 47 Corbin, J. D. and Reimann, E. M. (1974) Assay of cyclic AMP-dependent protein kinases.
783 Methods Enzymol. **38**, 287-290

784 48 Kramer, A. and Schneider-Mergener, J. (1998) Synthesis and screening of peptide libraries on
785 continuous cellulose membrane supports. Methods Mol Biol. **87**, 25-39

786 49 Carpentier, G. and Henault, E. (2010) Protein Array Analyzer for ImageJ. In Proceedings of
787 the ImageJ User and Developer Conference ed.)^eds.). pp. 238-240, Centre de Recherche Public Henri
788 Tudor

789 50 Solstad, T., Bjorgo, E., Koehler, C. J., Strozynski, M., Torgersen, K. M., Tasken, K. and
790 Thiede, B. (2010) Quantitative proteome analysis of detergent-resistant membranes identifies the
791 differential regulation of protein kinase C isoforms in apoptotic T cells. Proteomics. **10**, 2758-2768

792 51 Keryer, G., Alsat, E., Taskén, K. and Evain Brion, D. (1998) Role of cyclic AMP-dependant
793 protein kinases in human villous cytotrophoblast differentiation. Placenta. **19 Suppl 2**, S295-314

794 52 TenBroek, E. M., Lampe, P. D., Solan, J. L., Reynhout, J. K. and Johnson, R. G. (2001)
795 Ser364 of connexin43 and the upregulation of gap junction assembly by cAMP. J Cell Biol. **155**,
796 1307-1318

797 53 Shi, Q. J., Lei, Z. M., Rao, C. V. and Lin, J. (1993) Novel role of human chorionic
798 gonadotropin in differentiation of human cytotrophoblasts. Endocrinology. **132**, 1387-1395

799 54 Thevenin, A. F., Kowal, T. J., Fong, J. T., Kells, R. M., Fisher, C. G. and Falk, M. M. (2013)
800 Proteins and mechanisms regulating gap-junction assembly, internalization, and degradation.
801 Physiology (Bethesda). **28**, 93-116

802 55 Darrow, B. J., Fast, V. G., Kleber, A. G., Beyer, E. C. and Saffitz, J. E. (1996) Functional and
803 structural assessment of intercellular communication. Increased conduction velocity and enhanced
804 connexin expression in dibutyryl cAMP-treated cultured cardiac myocytes. Circ Res. **79**, 174-183

805 56 Paulson, A. F., Lampe, P. D., Meyer, R. A., TenBroek, E., Atkinson, M. M., Walseth, T. F.
806 and Johnson, R. G. (2000) Cyclic AMP and LDL trigger a rapid enhancement in gap junction
807 assembly through a stimulation of connexin trafficking. J Cell Sci. **113 (Pt 17)**, 3037-3049

808 57 Solan, J. L. and Lampe, P. D. (2014) Specific Cx43 phosphorylation events regulate gap
809 junction turnover in vivo. FEBS Lett. **588**, 1423-1429

810 58 Kennelly, P. J. and Krebs, E. G. (1991) Consensus sequences as substrate specificity
811 determinants for protein kinases and protein phosphatases. J Biol Chem. **266**, 15555-15558

812 59 Ruppelt, A., Oberprieler, N. G., Magklaras, G. and Tasken, K. (2009) Physiological substrates
813 of PKA and PKG. In Part II: Transmission: effectors and cytosolic events (2/E, H. o. c. s., ed.). pp.
814 1497-1514, Academic Press, La Jolla

815 60 Shah, M. M., Martinez, A. M. and Fletcher, W. H. (2002) The connexin43 gap junction
816 protein is phosphorylated by protein kinase A and protein kinase C: in vivo and in vitro studies. Mol
817 Cell Biochem. **238**, 57-68

818 61 Britz-Cunningham, S. H., Shah, M. M., Zuppan, C. W. and Fletcher, W. H. (1995) Mutations
819 of the Connexin43 gap-junction gene in patients with heart malformations and defects of laterality.
820 The New England journal of medicine. **332**, 1323-1329

821 62 Solan, J. L., Marquez-Rosado, L., Sorgen, P. L., Thornton, P. J., Gafken, P. R. and Lampe, P.
822 D. (2007) Phosphorylation at S365 is a gatekeeper event that changes the structure of Cx43 and
823 prevents down-regulation by PKC. J Cell Biol. **179**, 1301-1309

824 63 Lampe, P. D. (1994) Analyzing phorbol ester effects on gap junctional communication: a
825 dramatic inhibition of assembly. J Cell Biol. **127**, 1895-1905

826 64 Saez, J. C., Nairn, A. C., Czernik, A. J., Fishman, G. I., Spray, D. C. and Hertzberg, E. L.
827 (1997) Phosphorylation of connexin43 and the regulation of neonatal rat cardiac myocyte gap
828 junctions. Journal of molecular and cellular cardiology. **29**, 2131-2145

829 65 Yogo, K., Ogawa, T., Akiyama, M., Ishida, N. and Takeya, T. (2002) Identification and
830 functional analysis of novel phosphorylation sites in Cx43 in rat primary granulosa cells. FEBS Lett.
831 **531**, 132-136

832 66 Park, D. J., Wallick, C. J., Martyn, K. D., Lau, A. F., Jin, C. and Warn-Cramer, B. J. (2007)
833 Akt phosphorylates Connexin43 on Ser373, a "mode-1" binding site for 14-3-3. Cell Commun Adhes.
834 **14**, 211-226

835 67 Yogo, K., Ogawa, T., Akiyama, M., Ishida-Kitagawa, N., Sasada, H., Sato, E. and Takeya, T.
836 (2006) PKA implicated in the phosphorylation of Cx43 induced by stimulation with FSH in rat
837 granulosa cells. J Reprod Dev. **52**, 321-328

838 68 Dunn, C. A. and Lampe, P. D. (2014) Injury-triggered Akt phosphorylation of Cx43: a ZO-1-
839 driven molecular switch that regulates gap junction size. J Cell Sci. **127**, 455-464

840 69 Dunn, C. A., Su, V., Lau, A. F. and Lampe, P. D. (2012) Activation of Akt, not connexin 43
841 protein ubiquitination, regulates gap junction stability. J Biol Chem. **287**, 2600-2607

842 70 Park, D. J., Freitas, T. A., Wallick, C. J., Guyette, C. V. and Warn-Cramer, B. J. (2006)
843 Molecular dynamics and in vitro analysis of Connexin43: A new 14-3-3 mode-1 interacting protein.
844 Protein Sci. **15**, 2344-2355

845 71 Rust, H. L. and Thompson, P. R. (2011) Kinase consensus sequences: a breeding ground for
846 crosstalk. ACS Chem Biol. **6**, 881-892

847 72 Ksiezak-Reding, H., Pyo, H. K., Feinstein, B. and Pasinetti, G. M. (2003) Akt/PKB kinase
848 phosphorylates separately Thr212 and Ser214 of tau protein in vitro. Biochim Biophys Acta. **1639**,
849 159-168

850 73 Evans, G. J., Barclay, J. W., Prescott, G. R., Jo, S. R., Burgoyne, R. D., Birnbaum, M. J. and
851 Morgan, A. (2006) Protein kinase B/Akt is a novel cysteine string protein kinase that regulates
852 exocytosis release kinetics and quantal size. J Biol Chem. **281**, 1564-1572

853 74 Langbein, M., Strick, R., Strissel, P. L., Vogt, N., Parsch, H., Beckmann, M. W. and Schild, R.
854 L. (2008) Impaired cytotrophoblast cell-cell fusion is associated with reduced Syncytin and increased
855 apoptosis in patients with placental dysfunction. Molecular reproduction and development. **75**, 175-
856 183

857 75 Gauster, M., Moser, G., Orendi, K. and Huppertz, B. (2009) Factors involved in regulating
858 trophoblast fusion: potential role in the development of preeclampsia. Placenta. **30 Suppl A**, S49-54

859 76 Chen, C. P. (2014) Placental villous mesenchymal cells trigger trophoblast invasion. Cell Adh
860 Migr. **8**, 94-97

861 77 Boeldt, D. S., Yi, F. X. and Bird, I. M. (2011) eNOS activation and NO function: pregnancy
862 adaptive programming of capacitative entry responses alters nitric oxide (NO) output in vascular
863 endothelium--new insights into eNOS regulation through adaptive cell signaling. J Endocrinol. **210**,
864 243-258

865

Figure legends

Figure 1: PKA phosphorylates Cx43 and triggers human trophoblast fusion. (**A**) Trophoblasts were treated for 48 h with Arg-tagged cell-permeable PKI peptide or corresponding scrambled control. Cells were stained for desmoplakin (magenta) and nuclei (DAPI, cyan, left panels), and corresponding mononuclear cells with fusion indices were calculated as described in Experimental section (middle histograms). Levels of hCG and hPL secreted into the medium were also assayed and are shown as relative to scrambled control (right histograms). Scale bar: 30 μm. (**B**) Trophoblasts cultured with PKI or scrambled PKI and treated simultaneously with or without 8-CPT-cAMP (for 60 min) were examined by immunoblot for unphosphorylated (P0) and phosphorylated (P1/P2) Cx43, ezrin, phosphorylation of PKA-substrates (with a specific phospho-PKA substrate antibody) and actin (left panels). Ratio of unphosphorylated (P0) and phosphorylated (P1/P2) Cx43 expression was assessed by densimetric scanning of immunoblots (right histograms). (**C**) Trophoblasts were cultured for 24 h with PKI or corresponding scrambled control, treated with or without 8-CPT-cAMP for 60 min and subjected to PLA. Cells were stained with a pair of antibodies to Cx43 and desmoplakin. Physical proximity of the molecules was assessed using Duolink technology, generating spots when molecular proximity was < 40 nm. Scale bar: 30 μm. The intensity of the fluorescent spots generated were normalized to the number of nuclei and indicated in the corresponding histograms (right panel). Results are expressed as mean ± SEM of n = 3 independent experiments (ns for non-significant, * p <0.05, *** p < 0.001 as compared to control).

Figure 2: Ezrin organizes a complex that includes PKA and Cx43 in human trophoblasts. (**A**) Lysates from trophoblasts were subjected to immunoprecipitation (IP) with antibodies against ezrin, Cx43, PKA Cα, PKA RIα, PKA RIIα and non-specific IgG controls. Immunoprecipitates, IgG controls and corresponding lysates were analyzed by immunoblotting for the presence of the indicated proteins. Arrowheads indicate proteins of interest. (**B**) Physical proximity of ezrin-PKA RIα, ezrin-PKA RIIα, ezrin-PKA Cα, ezrin-Cx43, Cx43-PKA RIα, Cx43-PKA RIIα, Cx43-PKA-Cα complexes and non-specific IgG controls (mouse and rabbit) were assessed by PLA. Scale bar: 30 μm. (**C**) Lysates from trophoblasts were subjected to immunoprecipitation with antibodies against ezrin, Cx43, PKA Cα and

non-specific IgG controls. Immunoprecipitates and IgG control were assayed for cAMP-dependent (PKA) phosphotransferase activity with or without PKI as indicated in the histogram. Results are expressed as mean ± SEM of n = 3 independent experiments (ns for non-significant, * $p < 0.05$, ** $p < 0.01$, *** $p < 0.001$ as compared to respective control, $^{\#}$ $p < 0.05$, $^{\#\#}$ $p < 0.01$ as compared to IgG control).

Figure 3: Delineation of PKA phosphorylation sites in Cx43. (**A**) Level of *in vitro* phosphorylation by PKA of peptides with consensus PKA phosphorylation site (*i.e.* AAARRRRSFIFDAAA), from CREB with PKA phosphorylation site (*i.e.* AAARRPSYRKILNDL), from Cx43 with potential phosphorylation sites (*i.e.*VDQRPSSRASSRASSRPR) or peptide with consensus CK1D phosphorylation site (*i.e.* AAEEDAGSIFGFFAA) and quantified from phospho-peptide arrays pictured below histograms (Supplementary Figure S2). Data are presented as relative to the level of PKA phosphorylation of the peptide with the PKA consensus phosphorylation site. (**B-C**) Histograms represent the level of PKA phosphorylation of the wild type Cx43 peptide sequence encompassing amino acids 359 to 376 (WT) and in which single (**B**) or double combination (**C**) of serine substitution with alanine were made as indicated. Results are expressed as mean ± SEM of n = 4 independent experiments (*** $p < 0.001$). (**D**) Precipitated proteins from IAR20 cells with our without 8-CPT-cAMP treatment were subjected to immunoprecipitation with a Cx43-specific antibody and identified by nanoLC-LTQ Orbitrap mass spectrometry analysis of tryptic digests of bands excised from polyacrylamide gels after SDS-PAGE. Uniprot. Acc. No, accession number; #Pep, exclusive unique peptide count; #Spec, exclusive spectrum count; %Cov, percentage of amino acids identified; MW, molecular weight. (**E**) Phospho-peptides from the extreme C-terminal region of Cx43 identified by nanoLC-LTQ Orbitrap mass spectrometry from precipitated proteins as in (D). Phosphorylated serines are indicated in red.

Figure 4: Phospho-mimicking variants of Cx43 locate in gap junctions at the plasmalemma of human trophoblasts. (**A**) Trophoblasts were transfected with GFP-Cx43 variants. Cells were next stained with pairs of antibodies to GFP and desmoplakin and subjected to proximity ligation *in vitro*

assay (PLA). The interaction of molecules stained with pairs of antibodies was then assessed using Duolink technology. Magenta dots show molecular proximity (< 40 nm). Nuclei were counterstained with DAPI (cyan). Yellow pictures show GFP-tagged cell distribution. Merged pictures display duolink together with GFP-tagged cell distribution pictures. Scale bar: 30 μm. (**B**) Histograms represent the intensity of the dot signals normalized by the number of nuclei. Results are expressed as mean ± SEM of n = 3 independent experiments (* $p < 0.05$, ** $p < 0.01$, *** $p < 0.001$).

Figure 5: Trophoblast fusion is rescued by variants of Cx43 that mimic phosphorylation of S369 and S373. (**A**) Trophoblasts were transfected with Cx43 siRNA or scrambled control alone or together with mammalian expression vectors directing the expression of siRNA-resistant GFP-Cx43 (GFP-Cx43*), GFP-Cx43* R370E fusion protein without ability to bind to ezrin or GFP-Cx43* R370E with substitutions in the PKA phosphorylation region (GFP-Cx43* R370E 6SA or GFP-Cx43* R370E 6SD) or with individual phosphorylation-mimicking S to D and S to A substitutions in residues 364, 369, 373 or in combination for residues 369 and 373. Cells were next subjected to immunoblot analysis with the indicated antibodies. (**B**) Cells with Cx43 knockdown and/or reconstitution as in A were stained for desmoplakin (magenta) and nuclei (DAPI, cyan). Yellow shows GFP-tagged cells. Scale bar: 30 μm. (**C**) Histograms represent remaining mononuclear cells and fusion indices of treated-culture as in A and B. (**D**) Levels of hCG and hPL secreted into the medium of corresponding cultures were also assayed and are shown are relative to scrambled control. (**E**) Levels of hCG secreted into the medium were assayed from cultures of trophoblasts with Cx43 knockdown and reconstitution as in A and incubated with scrambled PKI or PKI. Results are expressed as mean ± SEM of n = 3 independent experiments (ns for non-significant, * $p < 0.05$, ** $p < 0.01$, *** $p < 0.001$).

Figure 6: Phosphorylation of residues 369 and/or 373 of Cx43 promotes gap junction communication. (**A**) HEK293 cells were transfected with mammalian expression vectors directing the expression of green fluorescent protein (GFP-control), or siRNA-resistant GFP-Cx43 (GFP-Cx43*), GFP-Cx43* R370E fusion protein without ability to bind to ezrin or GFP-Cx43* R370E with

949 individual phosphorylation-mimetic S to D and S to A substitutions in residues 369 (GFP-Cx43*
950 R370E S369A or GFP-Cx43* R370E S369D), 373 (GFP-Cx43* R370E S373A or GFP-Cx43* R370E
951 S373D) or in combination for both residues (GFP-Cx43* R370E S369-373A or GFP-Cx43* R370E
952 S369-373D) and subjected to FLIP experiments. GFP fluorescence intensity images of transfected
953 cells (left column) with C1 (*i.e.* dashed line) as the targeted cell by repetitive light beam exposition
954 and C2 (*i.e.* solid line) as the connected neighbor cell (left column). Calcein fluorescence intensity loss
955 in individual cells was mapped to pseudocolors as indicated by the color-scale bar [*F*, in arbitrary units
956 (a.u.)] before (pre-bleach, t=0 min) and 600 s after (post-bleach) repetitive light beam exposure of C1.
957 Kymograms display the temporal evolution of the fluorescent intensity mapped to pseudocolor of C1
958 and C2. The graph represents the corresponding fluorescence loss of C1 and C2 *versus* time (right
959 column). Scale bar: 10 μm. (**B**) Histograms exhibit the amalgamated data of calcein dye mobile
960 fractions from transfected cells measured in 3 independent experiments from different cultures, each
961 analyzing > 6 cells. Results are expressed as mean ± SEM (ns for non-significant, ** $p < 0.01$, *** $p <$
962 0.001).
963
964

SUPPLEMENTARY INFORMATION TO:

Ezrin-anchored PKA phosphorylates serine 369 and 373 on connexin 43 to enhance gap junction assembly, communication and cell fusion

by

Aleksandra R. Dukic, Pascale Gerbaud, Jean Guibourdenche, Bernd Thiede, Kjetil Taskén & Guillaume Pidoux

Supplementary Figure Legends

Supplemental Figure S1: Desmoplakin and Cx43 co-distribute at the membrane and PLA of Cx43/ezrin complex in human trophoblasts. (**A**) Primary human trophoblasts were co-immunostained for desmoplakin and Cx43 (left panel). Nuclei were counterstained with DAPI (blue). Yellow arrowheads indicate co-distribution. Scale bar: 15 μm. (Right panel) Line plot profile shows cellular distribution of desmoplakin and Cx43 in human trophoblasts (corresponding to merge picture's dashed line) (**B**) Trophoblasts were cultured for 24 h with PKI or corresponding scrambled control (Sc PKI), with or without 8-CPT-cAMP stimulation for 90 min and subjected to PLA. Cells were stained with a pair of antibodies: Cx43-ezrin. Physical proximity of the molecules was assessed using Duolink technology, generating white spots when molecular proximity was < 40 nm. Scale bar: 30 μm. The intensity of the fluorescent spots generated were normalized to the number of nuclei and indicated on corresponding graphs (right panel). (**C**) Histograms correspond to the normalization of Proximity Ligation Assay performed in Figure 1E as the intensity of the fluorescent spots generated by proximity of indicated pair of antibodies normalized to the number of nuclei. Results are expressed as the mean ± SEM of n = 3 independent experiments (* $p < 0.05$, ** $p < 0.01$, *** $p < 0.001$).

Supplemental Figure S2: Identification of PKA phospho-residues in Cx43.

(**A**) The sequence encompassing amino acids 359 to 376 of Cx43 was synthesized on cellulose membranes as overlapping 18-mer peptides with or without phosphoserine substitutions by alanine. Filters were incubated with recombinant PKA Cα subunit and subjected to PKA activity assay. PKA phosphorylation level of each peptide was revealed on a phosphoimager (top left panel) and signal intensities were quantified with ImageJ (top right panel). The signal intensity corresponding to the level of PKA phosphorylation for each phosphopeptide was mapped to pseudocolors as indicated by the color-scale bar [*S.I*, in arbitrary units (a.u.)]. Each peptide was identified on the quantified-filter by a column (C) and a line (L) number. The amino acid sequence of identified peptide was indicated (bottom panel). Phosphoserines and corresponding alanine substitutions are marked in red and bold red highlighted letters respectively. White boxes indicate phospho-peptides with reduction in PKA phosphorylation level and the corresponding amino acid sequences are indicated with red arrows. (**B**) Histograms represent the level of PKA phosphorylation of the wild type Cx43 sequence encompassing amino acids 359-376 (WT) and in which quadruple or quintuple combinations of serine substitutions with alanine were performed and the CK1D consensus phosphorylation site sequence as negative control. Results are expressed as the mean ± SEM of n = 4 independent experiments (* $p < 0.05$, ** $p < 0.01$, *** $p < 0.001$).

Supplemental Figure S3: Spectra of identified phospho-peptides from Cx43-CT. Spectra of identified peptides presented in Fig. 2E corresponding to the Cx43-CT domain of IAR20 cells without (**A**) or with 8-CPT-cAMP acute stimulation (**B)**. The peak heights show the relative intensities of the corresponding fragmentation ions.

Supplemental Figure S4: Plasmalemma subcellular localization of Cx43 phospho-mimicking variants. (**A**) Trophoblasts were transfected with GFP-Cx43 variants. Cells were next stained with pairs of antibodies to GFP and desmoplakin and subjected to proximity ligation *in vitro* assay (PLA). The interaction of molecules stained with pairs of antibodies was then assessed using Duolink technology. Magenta dots show molecular proximity (< 40 nm). Nuclei were counterstained with

DAPI (cyan). Yellow pictures show GFP-tagged cell distribution. Merge pictures display duolink together with GFP-tagged cell distribution pictures. Scale bar: 30 μm. (**B**) Immunoblot analysis of Cx43 and actin levels in trophoblasts transfected with specific Cx43 siRNA or scrambled controls (left panel). Level of Cx43 was assessed by densitometric scanning of immunoblots and normalized to actin levels in the same blots (right panel). Results are expressed as the mean ± SEM of n = 3 independent experiments (*** $p < 0.001$). (**C**) Scatter plots show correlation analysis between fusion indices and levels of syncytial hormones (hCG and hPL). Fusion indices and hCG or hPL secretion corresponds to the x- and y-coordinate, respectively. Pearson's correlation coefficients (R) are indicated. **(D)** HEK293 cells were transfected with Cx43 siRNA together with mammalian expression vectors directing the expression of siRNA-resistant GFP-Cx43 (GFP-Cx43*) or GFP-Cx43* with alanine substitutions in position 369 and 373 combined (GFP-CX43* S369-373A). Cells were next subjected to immunoblot analysis with the indicated antibodies (left panel). Level of Cx43, pCx43 S373 was assessed by densitometric scanning of immunoblots and normalized to actin levels in the same blots (right panel). Results are expressed as the mean ± SEM of n = 3 independent experiments (ns for non-significant, * $p < 0.05$).

Supplemental Figure S5: Ezrin bound to Cx43 brings PKA in vicinity of gap junctions in primary human trophoblasts leading to gap junction communication. (**A**) Trophoblasts were co-transfected with Cx43 siRNA and with the indicated Cx43 variants as in Fig. 5 and subjected to immunoprecipitation (IP) with GFP-specific antibody and non-specific IgG controls. Lysates, precipitates and IgG controls were analyzed by immunoblotting for the presence of ezrin, PKA RIα, PKA RIIα, PKA Cα, Cx43 and GFP. Arrowheads indicate proteins of interest. **(B)** HEK293 cells were transfected with or without mammalian expression vectors directing the expression of siRNA-resistant GFP-Cx43 (GFP-Cx43*), GFP-Cx43* R370E fusion protein without ability to bind ezrin or the green fluorescent protein (GFP-control). Cells were next subjected to immunoblot analysis with the indicated antibodies. (**C**) HEK293 cells were transfected with mammalian expression vectors directing the expression of GFP-Cx43* R370E with substitutions in the PKA phosphorylation region

(GFP-Cx43* R370E 6SA or GFP-Cx43* R370E 6SD) or with individual phosphorylation-mimicking S to D and S to A substitutions in residue 364, and subjected to gap-FLIP experiments. GFP fluorescence intensity images of transfected cells (left column) with C1 (*i.e.* dashed line) as the targeted cell by repetitive light beam exposition and C2 (*i.e.* solid line) as the connected neighbor cell (left column). Calcein fluorescence intensity loss in individual cells was mapped to pseudocolors as indicated by the color-scale bar [*F*, in arbitrary units (a.u.)] before (pre-bleach, t=0 min) and 600 s after (post-bleach) repetitive light beam exposure of C1. Kymograms display the temporal evolution of the fluorescent intensity mapped to pseudocolor of C1 and C2. The graph represents the corresponding fluorescence loss of C1 and C2 versus time (right column). Scale bar: 10 μm.

Dukic et al., Figure 1

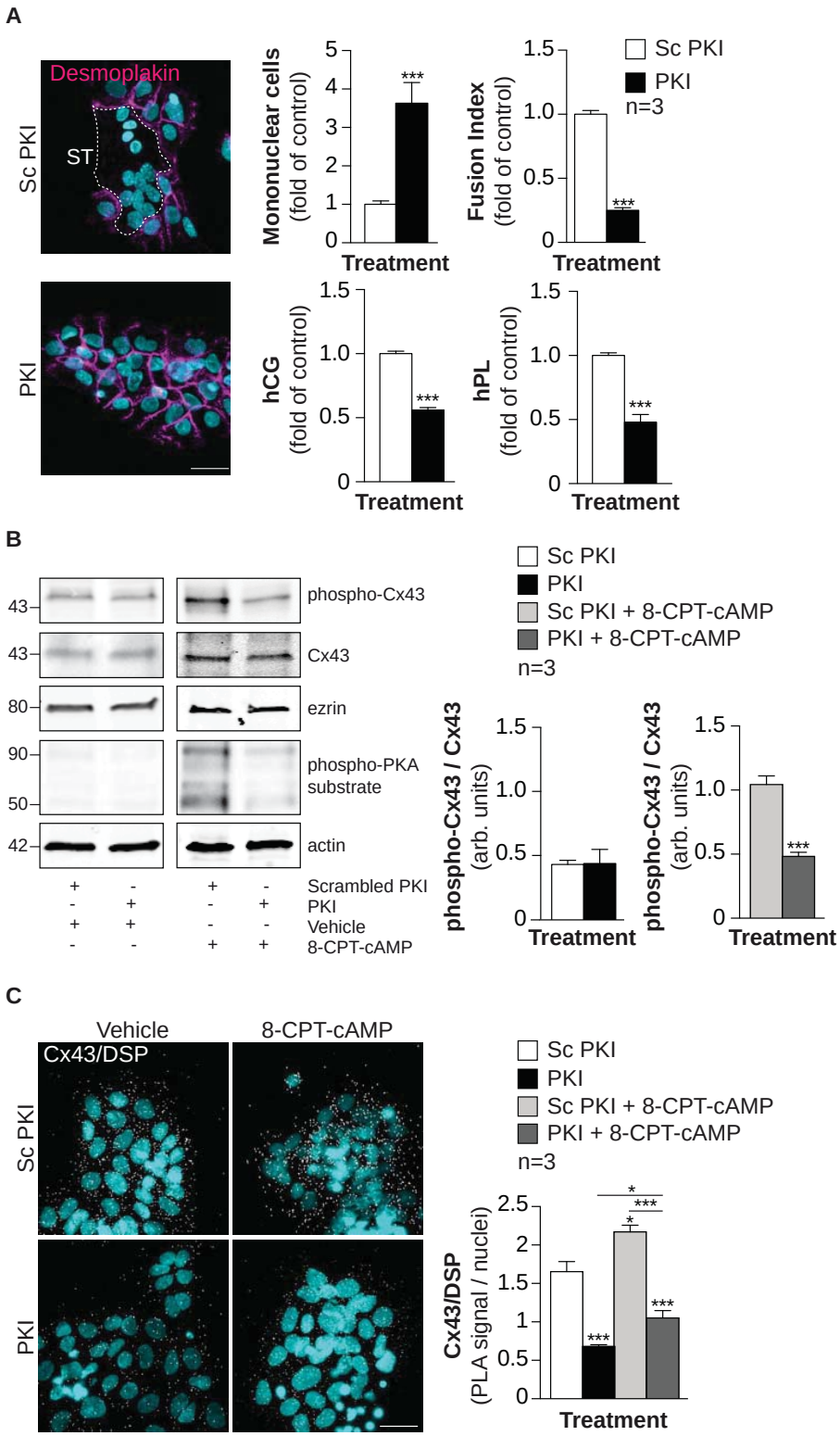

Dukic et al., Figure 2

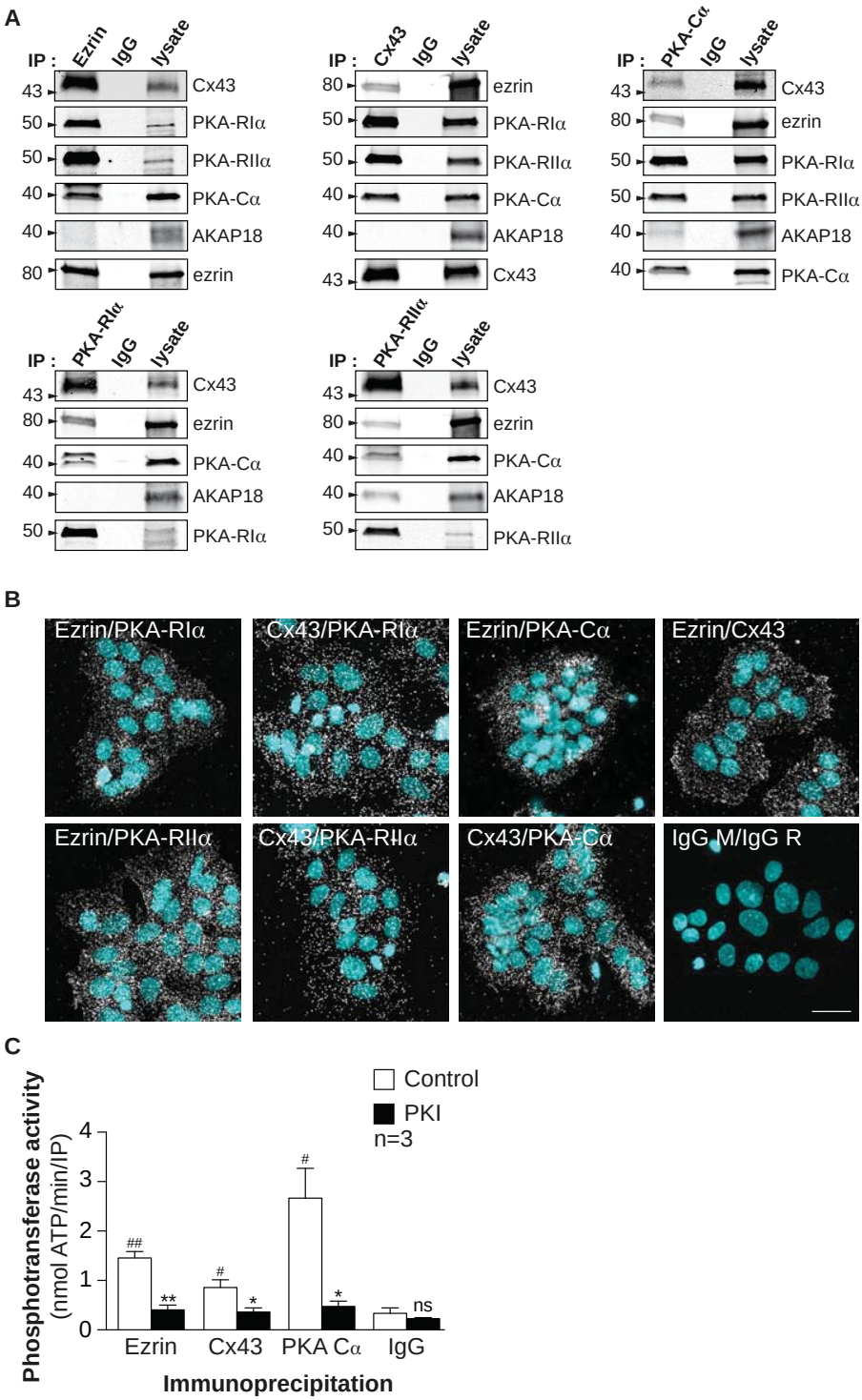

Dukic et al., Figure 3

A

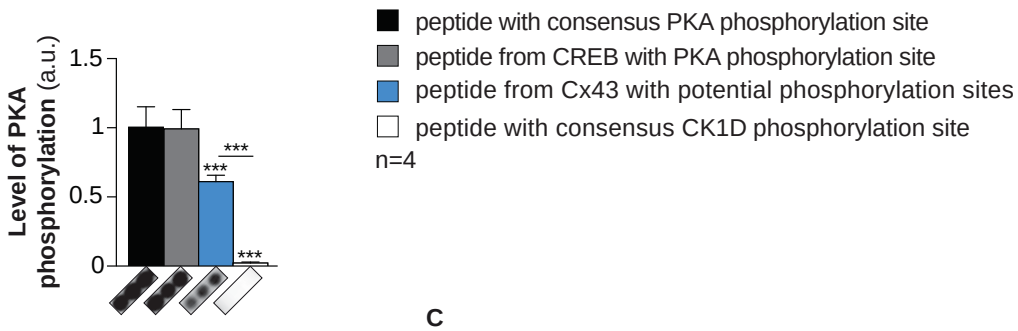

B

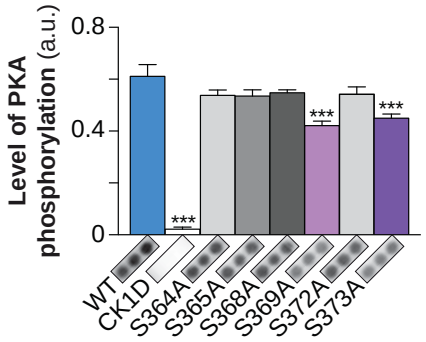

C

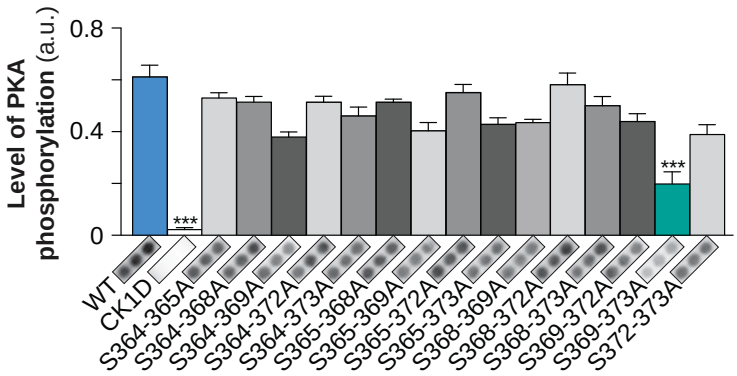

D

Cx43 Immunoprecipitation control

Protein name	UniProt. Acc. No.	# Pep	# Spec	% Cov	MW
Ezrin	P31977	5	8	7%	69 kDa
PKA Cα	P68182	3	3	11%	41 kDa
PKA RIIα	P12368	2	2	9%	46 kDa
Cx43	P08050	21	368	49%	43 kDa
Cx43 Immunoprecipitation + 8-CPT-cAMP					
Ezrin	P31977	11	19	19%	69 kDa
PKA Cα	P68182	2	2	8.3%	41 kDa
PKA RIα	P09456	2	2	7.9%	46 kDa
PKA RIIα	P12368	2	2	10%	46 kDa
Cx43	P08050	17	282	45%	43 kDa

E

Cx43 Immunoprecipitation control

Peptides	Modification	Mascot Ion Score	Mascot Delta ion Score	# Spec
(K)KVAAGHELQPLAIVDQRPSSR(A)	-	76	76	101
(K)KVAAGHELQPLAIVDQRPSSR(A)	phospho-S365	55	0	10
(K)VAAGHELQPLAIVDQRPSSR(A)	phospho-S364/365	45	45	1
(K)VAAGHELQPLAIVDQRPSSRASSR(A)	phospho-S365	26	0	1
(K)VAAGHELQPLAIVDQRPSSRASSR(A)	phospho-S364/365	14	3	1
(K)VAAGHELQPLAIVDQRPSSRASSR(A)	phospho-S365/368/369	15	0	1
(K)VAAGHELQPLAIVDQRPSSRASSR(A)	phospho-S365/369	12	0	1
(K)VAAGHELQPLAIVDQRPSSRASSR(A)	phospho-S369	7	0	1
(K)VAAGHELQPLAIVDQRPSSRASSR(A)	phospho-S368/369	2	0	1
(K)VAAGHELQPLAIVDQRPSSRASSR(A)	phospho-S364/369	4	0	1
(R)ASSRPRPDDLEI(-)	-	29	29	30
Cx43 Immunoprecipitation + 8-CPT-cAMP				
(K)KVAAGHELQPLAIVDQRPSSR(A)	-	82	82	82
(K)KVAAGHELQPLAIVDQRPSSR(A)	phospho-S365	39	0	3
(K)VAAGHELQPLAIVDQRPSSR(A)	phospho-S365	40	0	2
(K)VAAGHELQPLAIVDQRPSSR(A)	phospho-S364/365	22	22	1
(K)VAAGHELQPLAIVDQRPSSRASSR(A)	phospho-S368	26	0	1
(K)VAAGHELQPLAIVDQRPSSRASSR(A)	phospho-S369	10	0	3
(K)VAAGHELQPLAIVDQRPSSRASSR(A)	phospho-S365/368/369	7	0	2
(K)VAAGHELQPLAIVDQRPSSRASSR(A)	phospho-S365/368	6	3	1
(K)VAAGHELQPLAIVDQRPSSRASSR(A)	phospho-S368/369	5	0	2
(R)ASSRPRPDDLEI(-)	-	26	22	13
(R)ASSRPRPDDLEI(-)	phospho-S372/373	21	18	1

Dukic et al., Figure 4

A

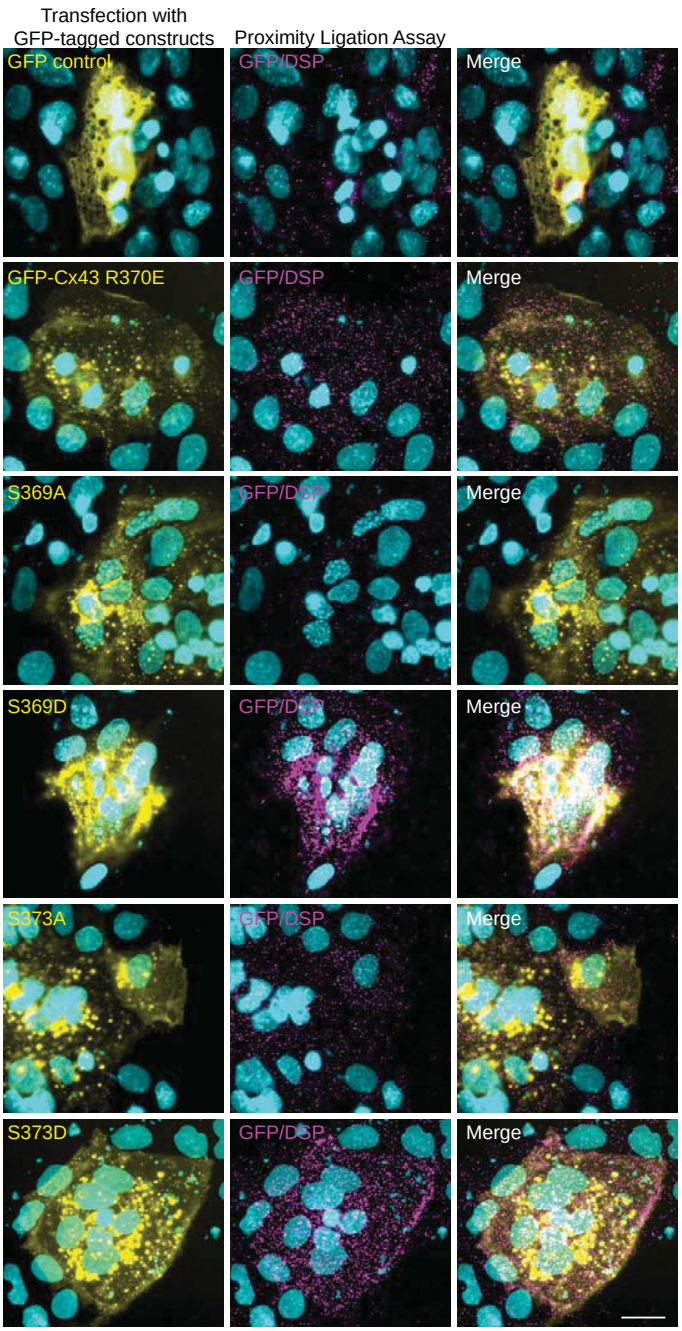

B

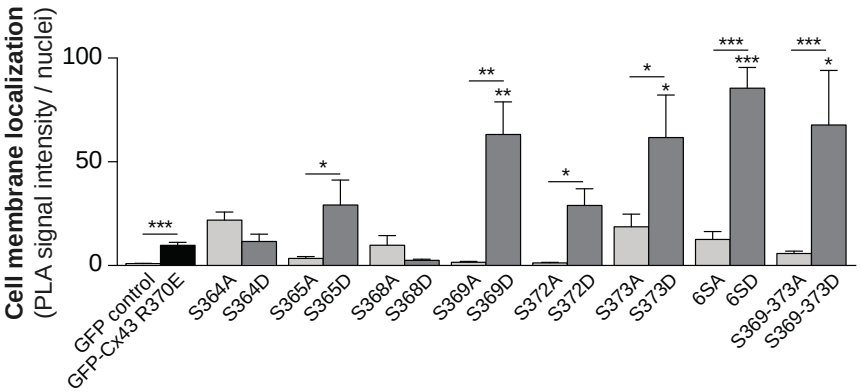

Dukic et al., Figure 5

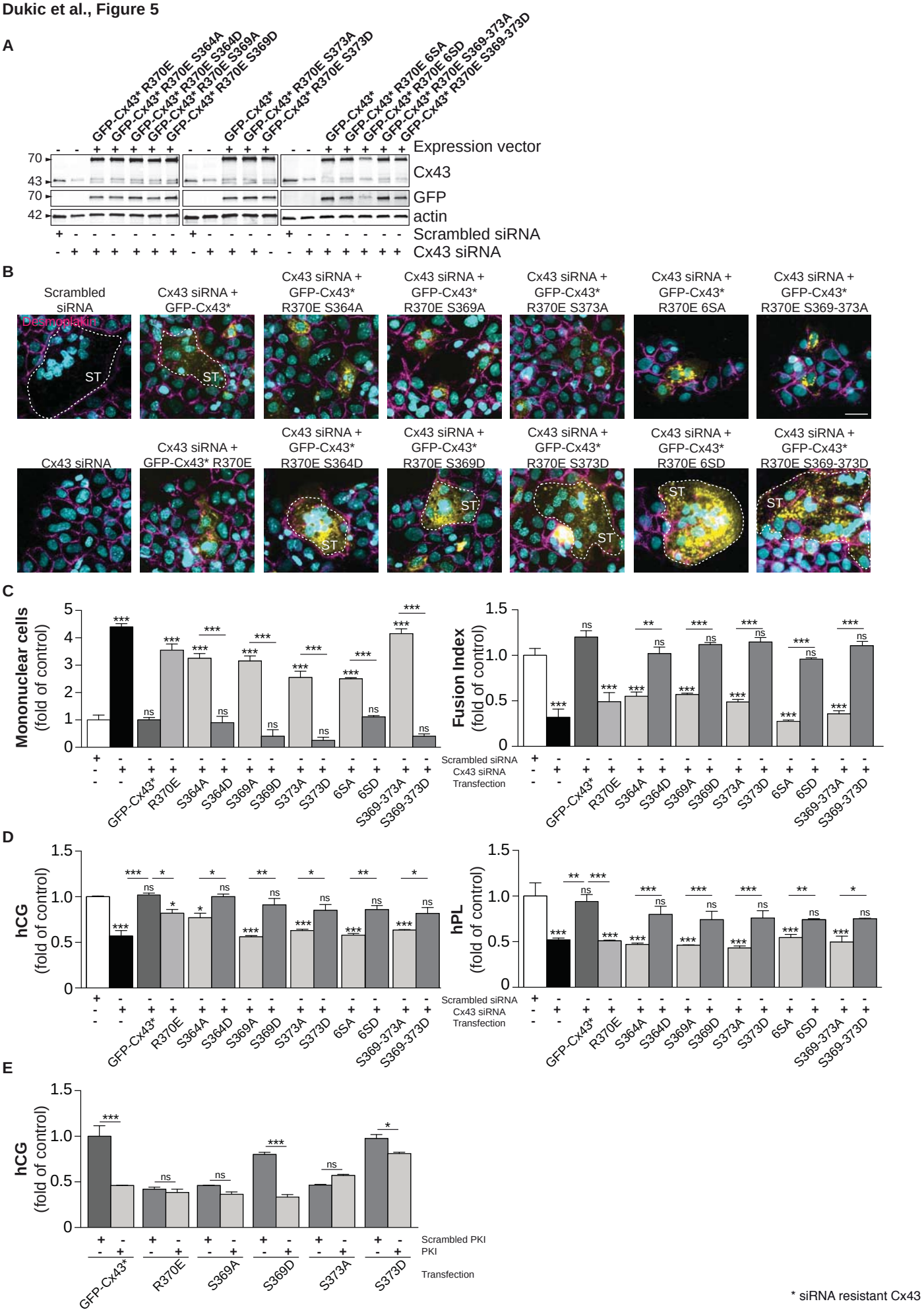

* siRNA resistant Cx43

Dukic et al., Figure 6

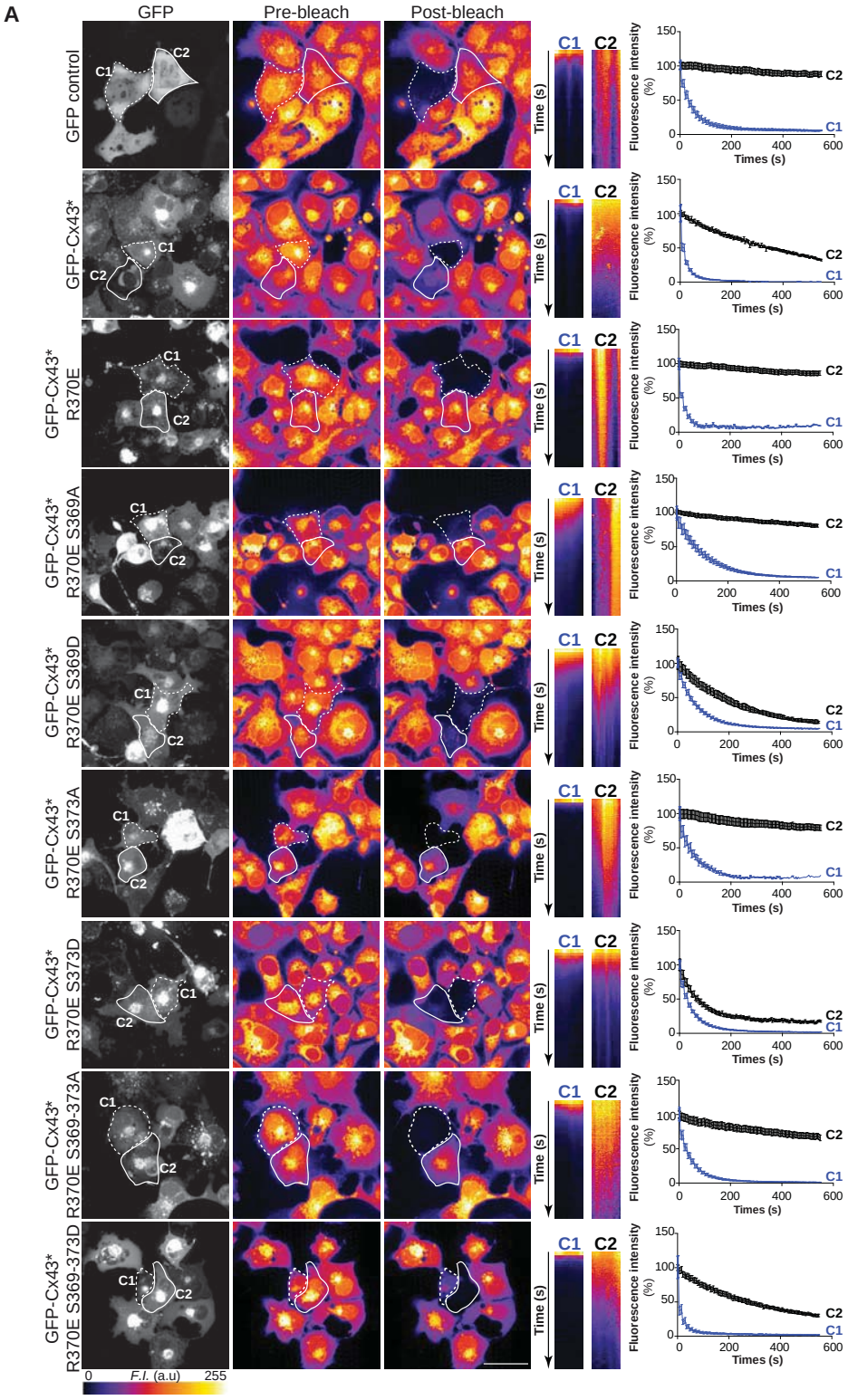

* siRNA resistant Cx43

Dukic et al., Supplementary Figure S1

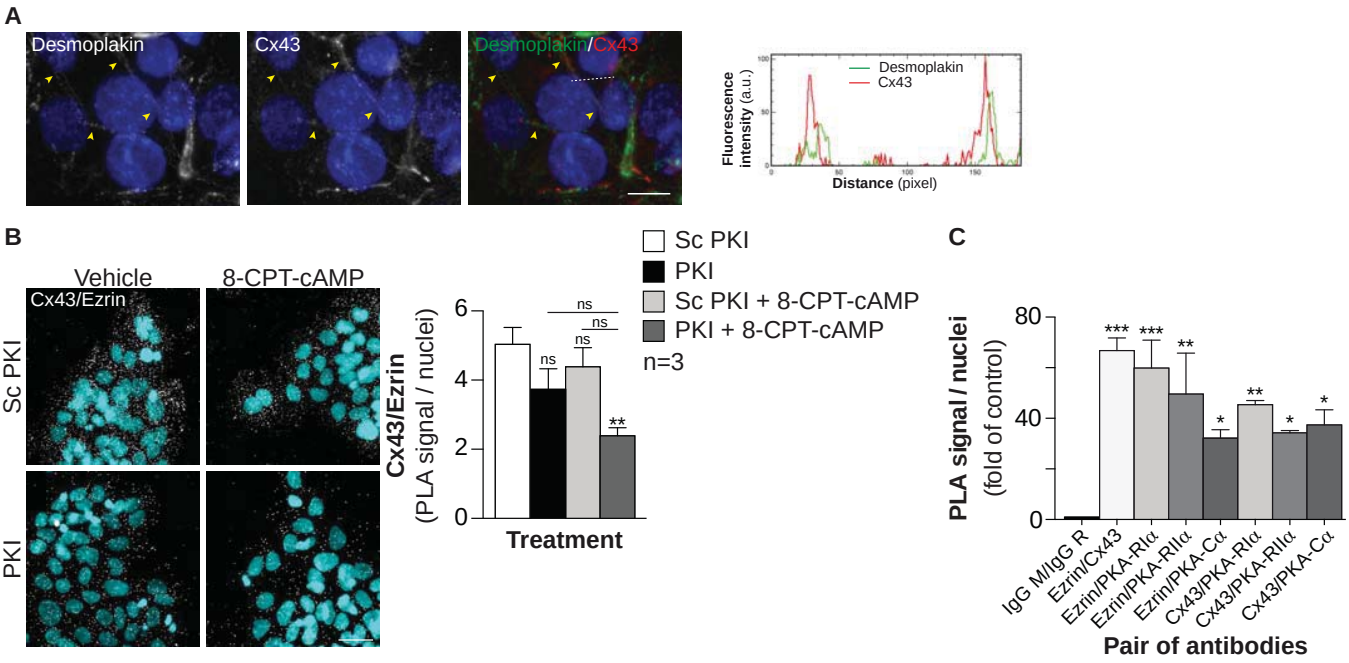

Dukic et al., Supplementary Figure S2

A

WT = ^{359}VDQRPSSRASSRASSRPR^{376}

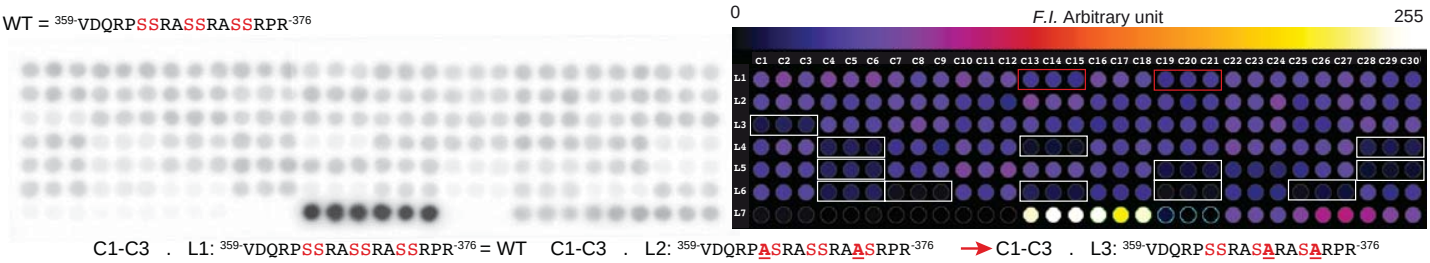

C1-C3 . L1: ^{359}VDQRPSSRASSRASSRPR^{376} = WT
C4-C6 . L1: ^{359}VDQRPASRASSRASSRPR^{376}
C7-C9 . L1: ^{359}VDQRPSARASSRASSRPR^{376}
C10-C12 . L1: ^{359}VDQRPSSRAASRASSRPR^{376}
→ C13-C15 . L1: ^{359}VDQRPSSRASARASSRPR^{376}
C16-C18 . L1: ^{359}VDQRPSSRASSRAASRPR^{376}
→ C19-C21 . L1: ^{359}VDQRPSSRASSRASARPR^{376}
C22-C24 . L1: ^{359}VDQRPAARASSRASSRPR^{376}
C25-C27 . L1: ^{359}VDQRPASRAASRASSRPR^{376}
C28-C30 . L1: ^{359}VDQRPASRASARASSRPR^{376}

C1-C3 . L2: ^{359}VDQRPASRASSRAASRPR^{376}
C4-C6 . L2: ^{359}VDQRPASRASSRASARPR^{376}
C7-C9 . L2: ^{359}VDQRPSARAASRASSRPR^{376}
C10-C12 . L2: ^{359}VDQRPSARASRASSRPR^{376}
C13-C15 . L2: ^{359}VDQRPSARASSRAASRPR^{376}
C16-C18 . L2: ^{359}VDQRPSARASSRASARPR^{376}
C19-C21 . L2: ^{359}VDQRPSSRAAARASSRPR^{376}
C22-C24 . L2: ^{359}VDQRPSSRAASRAASRPR^{376}
C25-C27 . L2: ^{359}VDQRPSSRAASRASARPR^{376}
C28-C30 . L2: ^{359}VDQRPSSRASARAASRPR^{376}

→ C1-C3 . L3: ^{359}VDQRPSSRASARASARPR^{376}
C4-C6 . L3: ^{359}VDQRPSSRASSRAAARPR^{376}
C7-C9 . L3: ^{359}VDQRPAARAASRASSRPR^{376}
C10-C12 . L3: ^{359}VDQRPASRAAARASSRPR^{376}
C13-C15 . L3: ^{359}VDQRPASRASARAASRPR^{376}
C16-C18 . L3: ^{359}VDQRPASRASSRAAARPR^{376}
C19-C21 . L3: ^{359}VDQRPAARASARASSRPR^{376}
C22-C24 . L3: ^{359}VDQRPAARASSRAASRPR^{376}
C25-C27 . L3: ^{359}VDQRPAARASSRASARPR^{376}
C28-C30 . L3: ^{359}VDQRPASRAASRAASRPR^{376}

C1-C3 . L4: ^{359}VDQRPASRAASRASARPR^{376}
→ C4-C6 . L4: ^{359}VDQRPASRASARASARPR^{376}
C7-C9 . L4: ^{359}VDQRPSARAAARASSRPR^{376}
C10-C12 . L4: ^{359}VDQRPSSRAAARAASRPR^{376}
→ C13-C15 . L4: ^{359}VDQRPSSRASARAAARPR^{376}
C16-C18 . L4: ^{359}VDQRPSARASARAASRPR^{376}
C19-C21 . L4: ^{359}VDQRPSARASSRAAARPR^{376}
C22-C24 . L4: ^{359}VDQRPSARAASRAASRPR^{376}
C25-C27 . L4: ^{359}VDQRPSARAASRASARPR^{376}
→ C28-C30 . L4: ^{359}VDQRPSARASARASARPR^{376}

C1-C3 . L5: ^{359}VDQRPSSRAASRAAARPR^{376}
→ C4-C6 . L5: ^{359}VDQRPSSRAAARASARPR^{376}
C7-C9 . L5: ^{359}VDQRPAARAAARASSRPR^{376}
C10-C12 . L5: ^{359}VDQRPAARAASRAASRPR^{376}
C13-C15 . L5: ^{359}VDQRPAARAASRASARPR^{376}
C16-C18 . L5: ^{359}VDQRPAARASARAASRPR^{376}
→ C19-C21 . L5: ^{359}VDQRPAARASARASARPR^{376}
C22-C24 . L5: ^{359}VDQRPAARASSRAAARPR^{376}
C25-C27 . L5: ^{359}VDQRPASRAAARASARPR^{376}
→ C28-C30 . L5: ^{359}VDQRPASRASARAAARPR^{376}

→ C1-C3 . L6: ^{359}VDQRPSARAAARAASRPR^{376}
→ C4-C6 . L6: ^{359}VDQRPSARAAARASARPR^{376}
→ C7-C9 . L6: ^{359}VDQRPSSRAAARAAARPR^{376}
C10-C12 . L6: ^{359}VDQRPSARAASRAAARPR^{376}
→ C13-C15 . L6: ^{359}VDQRPASRAAARASARPR^{376}
C16-C18 . L6: ^{359}VDQRPASRAASRAAARPR^{376}
→ C19-C21 . L6: ^{359}VDQRPSARASARASARPR^{376}
C22-C24 . L6: ^{359}VDQRPAARAAARAASRPR^{376}
→ C25-C27 . L6: ^{359}VDQRPAARAAARASARPR^{376}
C28-C30 . L6: ^{359}VDQRPAARAASRAAARPR^{376}

C1-C3 . L7: ^{359}VDQRPAARASARAAARPR^{376}
C4-C6 . L7: ^{359}VDQRPASRAAARAAARPR^{376}
C7-C9 . L7: ^{359}VDQRPSARAAARAAARPR^{376}
C10-C12 . L7: ^{359}VDQRPAARAAARAAARPR^{376}
C13-C15 . L7: AAARRRRSFIFDAAA = Consensus phospho-PKA
C16-C18 . L7: AAARRPSYRKILNDL = Phospho-CREB ^{133}S
C19-C21 . L7: AAEEDAGSIFGFFAA = Phospho-CK1D
C22-C24 . L7: ^{359}VDQRPSSRASSRASSRPR^{376} = WT
C25-C27 . L7: ^{359}VDQRPSSRASSRASSRPR^{376} = WT
C28-C30 . L7: ^{359}VDQRPSSRASSRASSRPR^{376} = WT

B

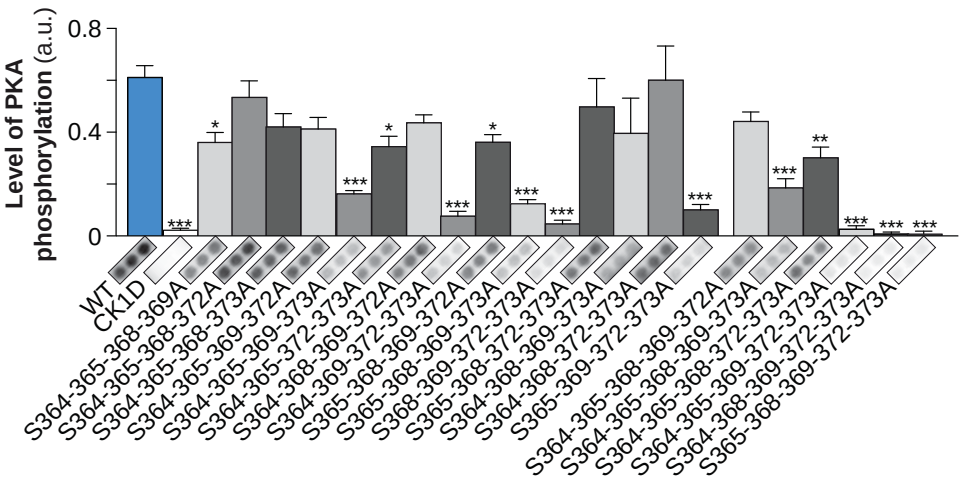

Dukic et al., Supplementary Figure S3

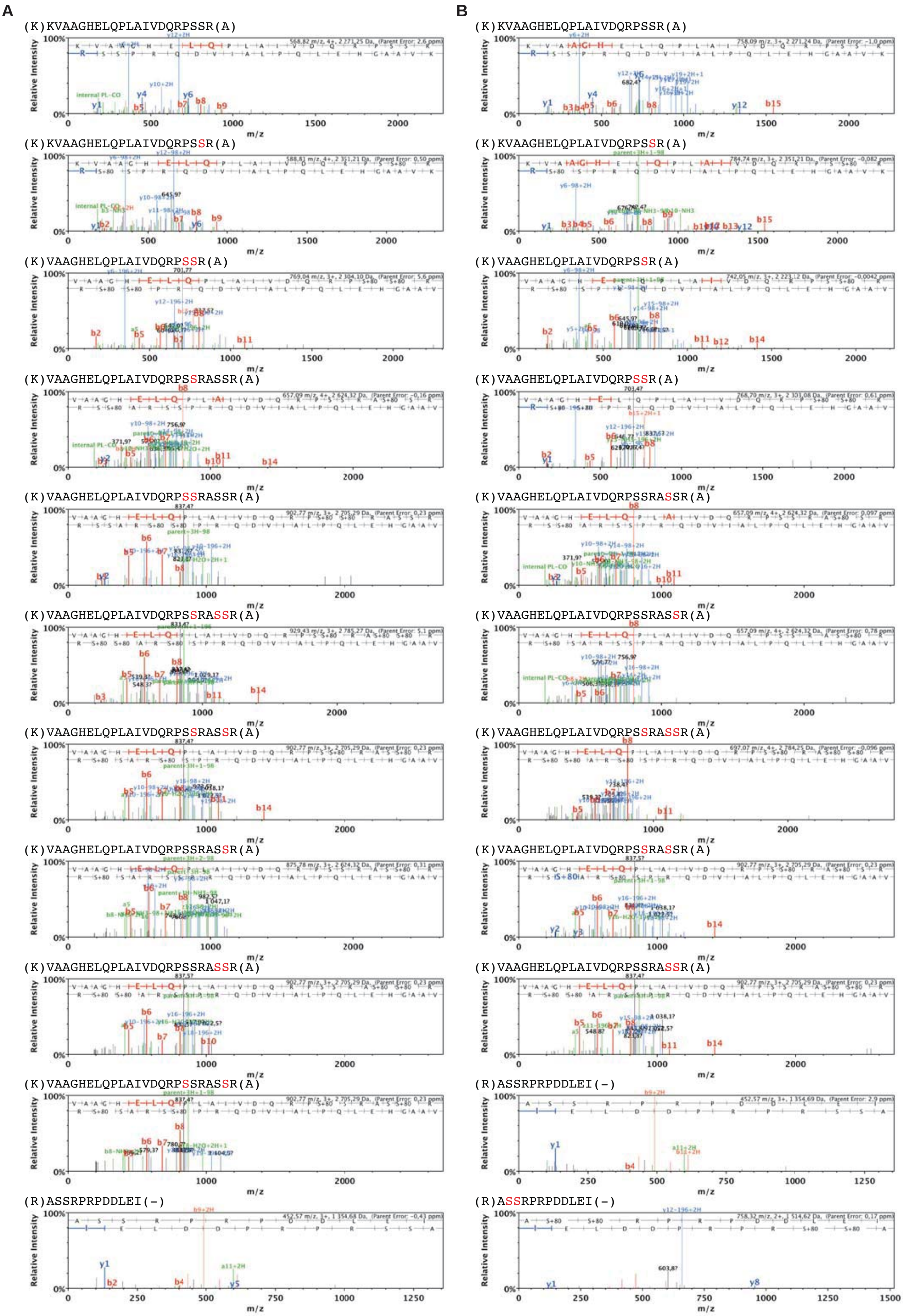

Dukic et al., Supplementary Figure S4

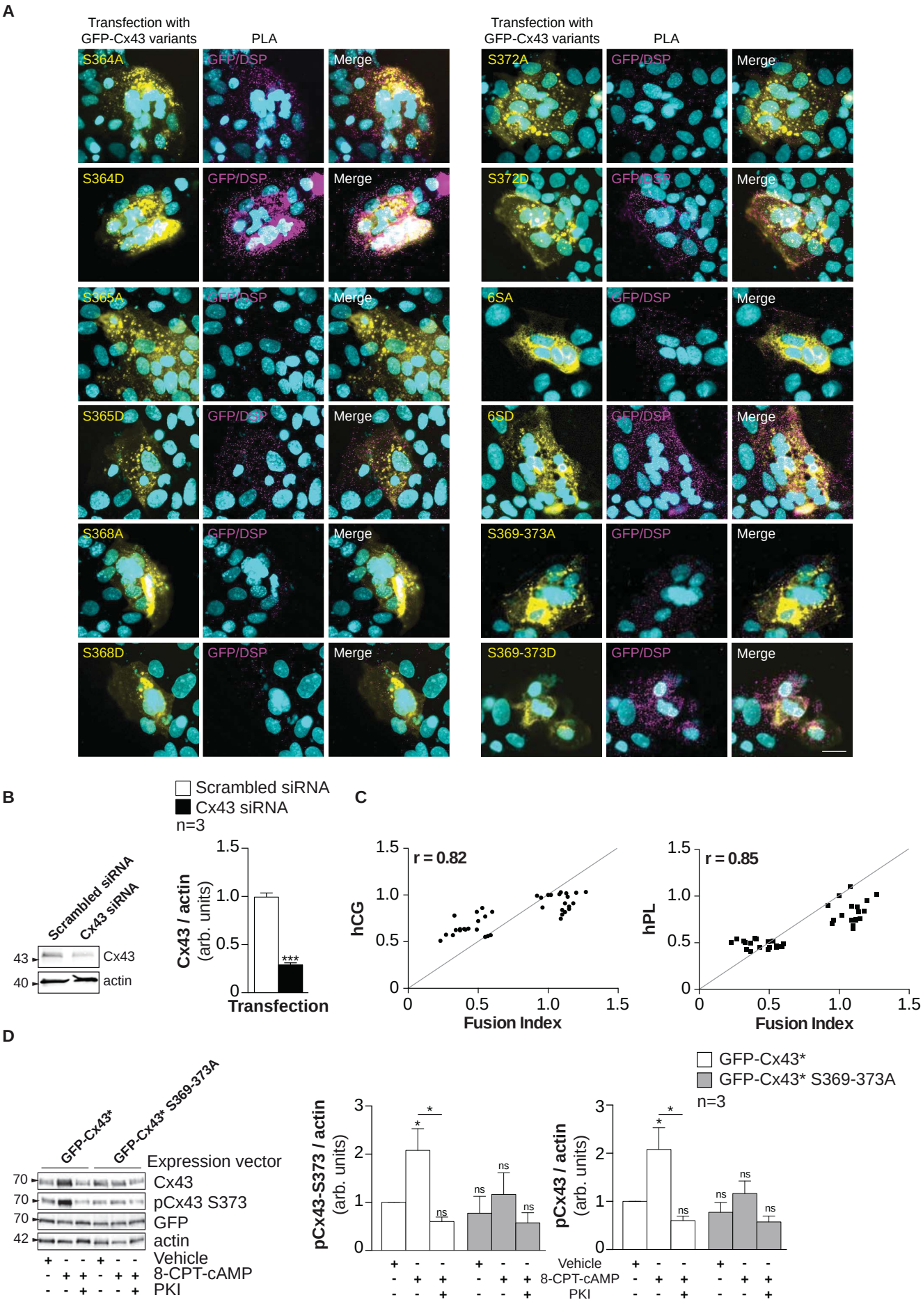

* siRNA resistant Cx43

Dukic et al., Supplementary Figure S5

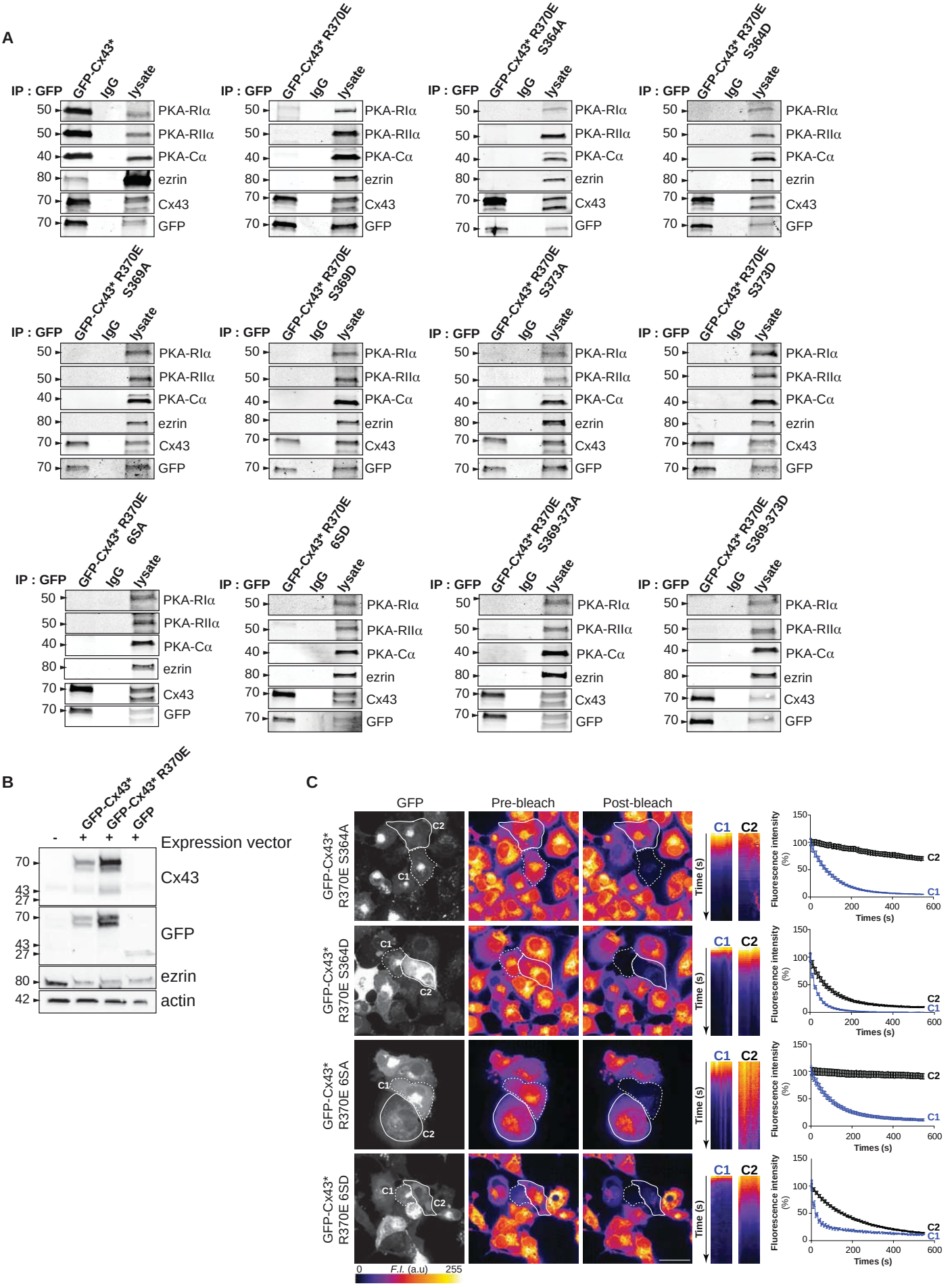

* siRNA resistant Cx43